1   ***Title:* Transcriptome landscape of a thermal-tolerant coral endosymbiont reveals**
2   **molecular signatures of symbiosis and dysbiosis**
3
4
5
6
7
8   **Anthony J. Bellantuono[a], Katherine E. Dougan[a], Camila Granados-Cifuentes[a,b],**
9   **and Mauricio Rodriguez-Lanetty[a]**
10
11   **[a]Department of Biological Sciences, Florida International University, Miami, FL**
12   **33199; [b]Baruch College—The City University of New York, New York, NY 10010**
13
14   **Corresponding Author: Mauricio Rodriguez-Lanetty (rodmauri@fiu.edu)**
15
16   **Keywords: coral bleaching, *Symbiodinium*, *Aiptasia*, symbiosis, dysbiosis,**
17   **transcriptomics, thermal tolerance**

Abstract

Background

Reef-building corals depend upon a nutritional endosymbiosis with photosynthetic dinoflagellates (family Symbiodiniaceae) for the vast majority of their energetic needs. While this mutualistic relationship is impacted by numerous stressors, heat stress from warming oceans is a predominant threat to coral reefs, placing the future of the world's reefs in peril due to climate change. While some Symbiodiniaceae species exhibit tolerance to thermal stress, the molecular basis for this tolerance is largely unexplored. To identify the underpinnings of heat tolerance and symbiosis, we compared the *in hospite* and free-living transcriptomes of *Durusdinium trenchii*, a pan-tropical heat-tolerant Symbiodiniaceae, under stable temperature conditions and acute hyperthermal stress.

Results

We discovered that under stable conditions, *in hospite* cells exhibited lower transcriptional activity than free-living counterparts, suggesting the shutdown of genes uniquely required for a free-living lifestyle in a process we term transcriptome reduction. However, under hyperthermal stress the transcriptional response was larger *in hospite* than in the free-living state, indicating an exacerbated stress environment within the host cell. While we identified a core heat stress response shared between free-living and *in hospite D. trenchii*, this represents only a minority of the stress-induced transcriptional activity. Our findings also revealed distinct processes at work in free-living and *in hospite* cells under non-stress conditions, with free-living *D. trenchii* exhibiting evidence of sexual reproduction. We also found that *in hospite* cells display putative host evasion activity including components of apicomplexan parasite invasion machinery.

Conclusions

In this work, we unraveled the molecular signatures of symbiont heat tolerance within the host, which is a critical step to enable the development of engineered endosymbionts as a tool for restoration of coral reefs. Our findings also highlight the necessity of conducting experiments on Symbiodiniaceae in the appropriate symbiotic state, as the stress responses of free-living cultures may not be representative of Symbiodiniaceae within a holobiont. We suggest that the necessity of an intermittent free-living state, outside of its highly co-evolved symbiosis, prevents genome reduction as seen in obligate endosymbionts. We posit that transcriptomic reduction of non-essential genes *in hospite* may be an alternative adaptive strategy for endosymbionts in ancient symbiotic assemblages.

Introduction

Reef-building corals engage in an obligate endosymbiosis with a diverse group of dinoflagellate algae in the family Symbiodiniaceae, which is composed of seven recently described genera (LaJeunesse et al., 2018). In this nutritional symbiosis, the algal partner transfers up to 90% of the carbon it fixes to the coral host (Muscatine et al., 1984). However, this critical mutualism is sensitive to environmental stressors and can break down in a process termed coral bleaching (Glynn, 1993), most commonly due to elevated seawater temperature linked to anthropogenic climate change (Hoegh-Guldberg, 1999). High temperature anomalies are continuing to intensify, with 2015–2016 exhibiting the most intense global bleaching event on record (Eakin et al., 2016; Hughes et al., 2017). Recent models forecast that mass bleaching will be an annual event before 2050 (Maynard et al., 2017). Even if dramatic international actions manage to limit warming to 1.5 °C, coral populations are predicted to remain in peril (Anthony et al., 2017).

There is an existing body of work demonstrating that the shift of the dominant symbiont (shuffling) or acquisition of new species of symbionts (switching) from the environment enables holobionts, the coral host and its diverse assemblage of symbionts, to better withstand climate-related increases in seawater temperatures (Baker, 2001; Berkelmans and Van Oppen, 2006; Jones et al., 2008; Rowan, 2004; Stat et al., 2006). More recently, significant differences in heat tolerance have been reported both within a single Symbiodiniaceae genus (Díaz-Almeyda et al., 2017) as well as between genera (Grégoire et al., 2017), revealing that different Symbiodiniaceae species have differing thermal optima and tolerances. A well-studied case is

3

79   *Durusdinium trenchii* (previously *Symbiodinium trenchii* [LaJeunesse et al., 2018]), an

80   ITS2 – D1a subtype within Clade D that has been shown to confer increases in heat

81   tolerance of between 1-1.5 °C to coral hosts (Berkelmans and Van Oppen, 2006;

82   Rowan, 2004). This heat tolerance is also observed in culture conditions; *D. trenchii* can

83   maintain maximum photosynthetic rates at elevated temperatures in comparison to the

84   majority of other investigated Symbiodiniaceae species (Grégoire et al., 2017).

85   However, alternate heat-resistant assemblages of host and symbiont come with a cost,

86   showing decreases in growth rates (Jones and Berkelmans, 2011; Little et al., 2004).

87   The potential benefits to corals hosting *D. trenchii* in response to increasingly

88   warm ocean conditions is not only evident in Pacific reef corals (Baker, 2003), where

89   this species of symbiont is genetically diverse and is thought to have originated, but

90   also in the Caribbean Sea, where it is thought to have invaded in the past half century

91   (Pettay et al., 2015). Silverstein et al. (2017) have demonstrated that the Caribbean

92   scleractinian coral *Montastraea cavernosa* colonized by *D. trenchii* persist *in hospite* on

93   thermally stressed reefs, whereas conspecific corals hosting type C3 symbionts

94   underwent massive bleaching.

95   Due to the current ecological crisis facing corals, there has been a growing

96   movement to develop purposeful interventions to increase the thermal tolerance of

97   many heat-sensitive coral holobionts, including experimental evolution and interspecific

98   hybridizations (Chakravarti et al., 2017; Chan et al., 2018). Recently, the use of genome

99   editing approaches has been proposed, with the primary goal of engineering heat-

100   sensitive endosymbionts in order to produce more heat-tolerant coral holobionts (Levin

101   et al., 2017). This requires the characterization of molecular mechanisms used by heat-

4

102   resistant Symbiodiniaceae species so that taxa exhibiting less resistant phenotypes can

103   be genetically engineered into heat-resistant symbionts.

104   By using a transcriptomic approach, we aimed to characterize the mRNA profiles

105   associated with the response to thermal stress in the heat-resistant *D. trenchii*. We

106   assessed the gene expression response of the symbiont both in the free-living state and

107   *in hospite* when stably associated with a cnidarian host. This design allowed us to

108   gauge the effect of symbiosis on the molecular response of the symbiont to heat stress.

109   In order to achieve sufficient sequencing depth of *in hospite D. trenchii*, we implemented

110   a novel symbiont mRNA enrichment technique. This powerful comparative approach

111   also facilitated an examination of the molecular changes underlying the transition from a

112   free-living to symbiotic state. This represents the first work to characterize the

113   transcriptional modifications associated with *in hospite* and free-living states of a

114   Symbiodiniaceae, and the first to characterize the divergent stress responses between

115   the symbiotic and free-living environment in a very ecologically important coral

116   symbiont, *D. trenchii*.

117   Our investigation reveals the dramatic differences in gene expression between

118   symbiotic and free-living *D. trenchii*. Further, we show that these differences are

119   magnified under conditions of thermal stress. When D. trenchii are in symbiosis, we

120   note a significant downregulation of transcripts. This molecular signature suggests that

121   the host provides a stabilized environment for *D. trenchii* in contrast to the free-living

122   state. Under thermal stress, the more active transcriptomic response of the

123   dinoflagellate *in hospite* in comparison to the free-living state suggests that the

124   dinoflagellates are responding to a less hospitable environment. This suggests that the

5

125   dinoflagellates living within host cells are responding to a more inhospitable

126   environment under thermal stress as disturbed host cells may intensify the stressful

127   state of the symbiont. This result brings critical attention to the necessity of examining

128   thermal stress responses of coral endosymbionts *in hospite* in order to capture the

129   functional profile actually relevant to coral holobiont persistence. Studies based solely

130   on free-living cultures provide a biased perspective that is confounded by responses to

131   an external environment markedly different from the holobiont.

132

Results and Discussion

133

Transcriptome Analysis

134

135   A reference transcriptome of 82,273 transcripts was assembled, filtered for non-

136   Symbiodiniaceae transcripts, and used as the basis for differential expression analysis

137   (NCBI TSA BioProject PRJNA508937). Principal component analysis (PCA) of all

138   analyzed transcripts shows dramatic separation of treatments by both symbiotic state as

139   well as thermal stress (Fig. 2*A*). PC1, the principal component separating *in hospite* and

140   free-living treatments, is driven by 11,933 transcripts and explains 40.5% of the

141   variance, whereas PC2, the axis separating thermal treatment, is driven by 11,904

142   transcripts and explains 15.5% of the variance.

143   Statistical analysis for the identification of differentially expressed transcripts

144   (FDR corrected p-value < 0.01, greater than $\log_2$ 2-fold difference) reveals that the *in*

145   *hospite* condition in *D. trenchii* is marked by a substantial downregulation of gene

146   expression, with 368 transcripts upregulated versus 1625 downregulated at the 28°C

147   (Fig. 3A). This larger level of downregulation *in hospite* is maintained under the heat

148   stress comparison (34°C), with 2799 transcripts downregulated versus 793 upregulated

149   in comparison to the free-living state (Fig. 3A). Notably, the *in hospite* response to heat

150   stress is much more pronounced than that in the free-living condition, with a total of 709

151   transcripts differentially regulated as a function of thermal stress *in hospite* versus 353

152   transcripts in the free-living condition (Fig. 3B). Out of the 709 transcripts involved in

153   the *in hospite* response to heat, 624 transcripts (365 upregulated and 259

154   downregulated) were specific to the *in hospite* condition as these transcripts were not

155   differentially expressed in response to thermal challenge in free-living *D. trenchii* (Fig.

156   3B). The transcriptional response to thermal stress shared between free-living and *in*

157   *hospite D. trenchii* represented only 12% of the heat-modulated transcriptional response

158   *in hospite.* This shared response could be considered the core heat response, with

159   activity regardless of the symbiotic state of the algal endosymbiont. However, this

160   represents a minority of detected transcriptional activity. The majority of transcripts

161   involved in response to heat stress depend upon the symbiotic condition of the

162   dinoflagellate (e.g. whether the cell is *in hospite* or free-living). Our findings demonstrate

163   that *D. trenchii* has distinct transcriptomic profiles *in hospite* and in free-living states,

164   and further, that the transcriptomic heat stress response is vastly different between *in*

165   *hospite* and free-living conditions. This brings critical attention to the importance of

166   examining the response of Symbiodiniaceae holistically, as the responses in culture

167   may not be representative of *in hospite* endosymbionts. To date, the vast majority of

168   transcriptomic assessments of Symbiodiniaceae within the context of thermal stress

169   have been performed exclusively on free-living cultures (Barshis et al., 2014;

170   Baumgarten et al., 2013; Díaz-Almeyda et al., 2017; Gierz et al., 2017; Levin et al.,

7

171   2016; Rachel Ashley Levin et al., 2017; Liew et al., 2017; Xiang et al., 2015), and while

172   they have been insightful, they may present a reduced transcriptional picture of the

173   alterations that occur in Symbiodiniaceae *in hospite*. Only one other investigation

174   directly compared gene expression *in hospite* to free-living conditions (Rosic et al.,

175   2010), but it focused on only two heat-shock protein genes. We propose that it is

176   imperative to consider the *in hospite* environment in the assessment of

177   Symbiodiniaceae response to thermal stress, and that culture-based studies require

178   careful consideration when extending findings to *in hospite* conditions.

179   **A Small Core Thermal Stress Response is Shared Between Free-living and *in***
180   ***hospite D. trenchii***
181
182   Within the conserved transcriptional changes under thermal stress shared

183   between the free-living and *in hospite* states of *D. trenchii* (Fig. 3, Fig. 4), 57 transcripts

184   were upregulated and 28 downregulated. Examination at the transcript level reveals that

185   the magnitude of expression within these core transcripts is, overall, higher in free-living

186   *D. trenchii* than *in hospite* (Fig. 4). With a relatively small number of transcripts

187   representing the core response, we were not able to perform meaningful GO term

188   enrichment analysis. Instead, our interpretation of this small conserved core response is

189   based upon transcript annotations.

190   Though the core set of transcripts differentially expressed in response to thermal

191   stress (Fig. 3) represents the minority of transcriptional alterations under stress *in*

192   *hospite* and in free-living cells, it sheds light on key processes conserved in the *D.*

193   *trenchii* stress response independent of symbiotic state. These processes include

194   modifications to membrane fluidity, DNA repair, anion channel activity, spermidine

195   synthase upregulation, and transposition. With their indispensability in both the *in*

8

196   *hospite* and free-living stress responses, these associated transcripts are potentially

197   important candidates in the identification of the genetic basis for thermal tolerance in *D.*

198   *trenchii.*

199   Maintenance of membrane viscosity is critical for cell homeostasis as

200   hyperthermal stress increases the fluidity of membranes, potentially leading to

201   disintegration of the lipid bilayer (Allakhverdiev et al., 2008). In Symbiodiniaceae,

202   thylakoid membrane lipid composition is a key determinant of thermal-stress sensitivity

203   (Tchernov et al., 2004). Within the core heat stress response, we identify an ortholog to

204   a *fatty acyl-CoA desaturase*, an enzyme involved in the remodeling of cell membranes

205   for homeoviscous adaptation (Hazel, 1995) that is potentially critical in modifying fluidity

206   to accommodate increasing temperatures.

207   The upregulation of *apurinic endonuclease-redox protein* (*ARP*) both *in hospite*

208   and in free-living conditions suggests that repair to oxidative DNA base damage occur

209   in both conditions. The apurinic/apyrimidinic (AP) endonucleases are important DNA

210   repair enzymes involved in two overlapping pathways: DNA glycosylase-initiated base

211   excision and AP endonuclease-initiated nucleotide incision repair (Akishev et al., 2016).

212   In the context of heat stress, this may allow *D. trenchii* a faster response to DNA

213   damage than other Symbiodiniaceae species.

214   Anion channels, spermidine synthase, and retrotransposons are disparate

215   entities which can each serve as heat stress response mediators with many

216   downstream effectors. In plants, anion channels are a master regulator of stress

217   response (reviewed by Rob et al., 2012). In the core heat stress response, we find the

218   upregulation of a transcript putatively coding for aluminum-activated malate transporter

9

219   9 (ALMT9). In plants, ALMT9 is involved in the release of chloride currents in guard

220   cells and malate homoeostasis. In response to stress, the release of chloride and

221   malate leads to the rapid stomatal closure (Dreyer et al., 2012). Though the precise role

222   of ALMT9 in stress response in Symbiodiniaceae species is unknown, it may be

223   involved in downstream stress response signaling. A transcript coding for spermidine

224   synthase is also upregulated across heat stress treatments. Spermidine synthase in

225   *Arabidopsis* dramatically improves stress tolerance when overexpressed via its effect on

226   multiple downstream targets (Kasukabe et al., 2004), while exogenous application of the

227   protein increases antioxidant tolerance in creeping bentgrass (Li et al., 2015). An

228   additional transcript of the core response potentially acting as an upstream effector of

229   numerous targets codes for LINE-1 reverse transcriptase. Recent work by Chen et al.

230   (2018) identified Ty1-copia-type LTR retrotransposons in *Symbiodinium microadriaticum*

231   which are activated by heat stress, suggesting that this may be a mechanism for the

232   generation of genetic variation under heat stress. Diatoms also possess stress-activated

233   retrotransposons, which are postulated to serves as generators of genetic variability

234   (Maumus et al., 2009). The involvement of retrotransposons in stress response has also

235   been observed across taxa. In plants, retrotransposons are activated by stress and go

236   on to activate numerous host regulatory pathways (Grandbastien, 2015, 1998).

237   **D. trenchii response to heat stress depends on the symbiotic state**
238
239   The majority (88% *in hospite* and 76% free-living) of the transcriptional response

240   to thermal stress is specific to the symbiotic state of the dinoflagellate (Fig. 3B). Both

241   free-living and *in hospite D. trenchii* have distinct responses to a thermal challenge of

242   34°C not only at the level of transcript identity (Fig. 3), but also with regard to enriched

243   gene ontology terms which are unique to each symbiotic state (Fig. 5). *In hospite D.*

244   *trenchii* have transcriptional activity with parent GO terms such as mRNA transport, N-

245   terminal protein amino acid acetylation, and cellular response to temperature stimulus,

246   all of which are not enriched in the free-living transcriptomic response to heat stress

247   (Fig. 5). There is also a striking *in hospite*-specific decrease in GO terms within the

248   category "binding of sperm to zona pellucida" under heat stress. In the case of the free-

249   living state, negative regulation of viral genome replication is highly downregulated in

250   contrast to the symbiotic state (Fig. 5). While the analysis reveals that the majority of

251   ontologies affected by heat stress are disparate depending upon symbiotic state,

252   decreased activity of vesicle-mediated transport is a common theme in the heat stress

253   response of both *in hospite* and free-living *D. trenchii* (Fig. 5). Despite this particular

254   instance of overlap in function indicated by gene ontology analysis, the transcripts

255   underlying vesicle-mediated transport in free-living and symbiotic treatments are distinct

256   in the symbiotic and free-living conditions (Supplement_2_DEGs_Annotations.xlsx).

257   Remarkably, despite the more highly responsive transcriptome of *in hospite D.*

258   *trenchii* to heat stress than free-living cells, free-living *D. trenchii* mount a more dramatic

259   response to photoxidative stress than *in hospite* at both 28°C and 34°C (Fig. 6). Gene

260   ontology terms for thermoception and response to oxidative stress are also highly

261   represented in free-living *D. trenchii* at 34°C, whereas no enrichment is detected *in*

262   *hospite* (Fig. 6). This suggests that the intracellular environment of the host provides

263   some level of protection for the endosymbiont from some aspects of photothermal

264   stress, potentially by a modified light environment within the host. This is supported by

265   earlier work by Bhagooli and collaborators (Bhagooli et al., 2008), who found that

11

266   multiple genera of Symbiodiniaceae exposed to photothermal stress *in hospite* had

267   unaffected photosynthetic output and less impact to maximum quantum yield in

268   comparison to cultured cells across genera. Coral hosts possess multiple mechanisms

269   for sheltering endosymbionts including photoprotective host chromoproteins (Dove et

270   al., 2001; Quick et al., 2018; Salih et al., n.d.; Smith et al., 2013) and other host-

271   mediated modifications to the internal light environment, such as scattering by the coral

272   skeleton (Enríquez et al., 2005; Wangpraseurt et al., 2012). While this sheltering *in*

273   *hospite* may, on its surface, appear contradictory, we posit that the *in hospite* state has

274   a more complex transcriptional response to thermal stress overall, but that the host may

275   reduce light stress.

276   By examining ontologies from differentially expressed transcripts exclusively

277   associated with free-living and *in hospite* treatments, we found that the *in hospite* heat

278   stress response is highly enriched for mRNA transport and cellular response to

279   temperature stimulus (Fig. 5). We suggest that host sheltering of *in hospite* cells light

280   may contribute to a symbiont's capacity to maintain some cellular functions which may

281   be heavily impacted in unsheltered free-living cells. This may result in the mounting of a

282   more effective transcriptional response to heat stress. Under acute thermal stress, yeast

283   block mRNA transport of transcripts uninvolved in the heat stress response (Saavedra

284   et al., 1996). If unsheltered free-living cells are under more severe stress, experiencing

285   the unfiltered brunt of light in combination with heat stress, mRNA transport may be

286   highly inhibited, as suggested by our analyses.

287   The *in hospite* state also exhibits a dramatic reduction in GO term enrichment

288   within the biological process binding of sperm to zona pellucida, a response not

289   observed in the free-living comparison (Fig. 5). One of the transcripts underlying this

290   enrichment (TRINITY_DN30024_c0_g1_i6) has high identity to *sperm surface protein*

291   *Sp17*, a protein possessed by sperm which binds the zona pellucida during mammalian

292   fertilization, critical for cell adhesion (O'rand et al., 1995; Richardson et al., 1994). The

293   expression of the putative *Sp17* ortholog may function in the mediation of normal

294   symbiosis, potentially involved in adhesion between the symbiont and host, while the

295   observed decrease in expression may be a part of dysbiosis.

296   Taken together, the intracellular environment experienced by *in hospite*

297   symbionts represents a complex set of interactions between the host, the external

298   environment, and the endosymbiont. The disparate transcriptomes of stress *in hospite*

299   and free-living likely result from a combination of protection from some aspects of stress

300   by the host, the complexity of an intracellular environment compared with that of a free-

301   living cell, and further, the transcriptional activity involved in the mediation of the

302   symbiosis, as discussed in sections that follow.

303   **Alterations required for the transition between free-living and symbiotic states**

304   Comparing the *in hospite* and free-living transcriptomes of *D. trenchii* provides a

305   window into the alterations necessary for symbiotic living. Several processes are

306   exclusively enriched *in hospite* under non-stress conditions at 28°C, in comparison to

307   the free-living state (28°C symbiotic vs. 28°C free-living) (Fig. 6). Late endosome to

308   vacuole transport and mRNA cis splicing via spliceosome are both highly enriched *in*

309   *hospite* along with response to prostaglandin F. The roles of increased lysosome activity

310   and enhanced cis splicing in symbiosis are unknown, but complexities in

311   Symbiodiniaceae mRNA splicing, including trans-splicing (Zhang et al., 2007) and non-

13

312   canonical intron splicing (Aranda et al., 2016; Lin, 2011; Mendez et al., 2015). The

313   enrichment of response to prostaglandin F is extremely curious as the highest

314   concentrations of prostaglandins are found in corals, where these compounds are

315   produced by the host (Valmsen et al., 2001; Weinheimer and Spraggins, 1969).

316   Hydrogen peroxide catabolism is enriched *in hospite* at both 28°C and 34°C in

317   comparison to the free-living state, with higher activity at 34°C. Increased scavenging of

318   hydrogen peroxide *in hospite* could potentially be adaptive and necessary for

319   maintaining stable symbiosis, as while the release of peroxide in the free-living state is

320   likely of minimal detriment, the release of this form of ROS *in hospite* is held to induce

321   an immune response on the part of the host (reviewed by Weis, 2008).

322   In addition to the aforementioned enrichment of photooxidative stress terms in

323   the free-living state under thermal challenge (34°C), the transcripts upregulated in the

324   free-living state at 28°C are also enriched for numerous terms associated with response

325   to photooxidative stress. While this is amongst the highest activity of parent GO terms in

326   the free-living condition at both thermal treatments, no increase in enrichment is found

327   in the *in hospite* condition at either 28°C or 34°C. Dipeptide transport as well as

328   heterochromatin organization are also highly enriched in the free-living condition at

329   28°C.

330   ***D. trenchii* exhibits transcriptome reduction *in hospite***

331   Genome reduction is a common phenomenon in obligate microbial

332   endosymbionts (Martínez-Cano et al., 2015; McCutcheon and Moran, 2012) which can

333   occur via multiple mechanisms. In obligate intracellular endosymbioses, there are some

334   common demographic conditions imposed upon the endosymbiont, namely relatively

14

335   small effective population size of endosymbionts, restriction to specific hosts, and

336   limited recombination between endosymbiont strains within the host (Martínez-Cano et

337   al., 2015). These conditions set the stage for genetic drift and loss of genes that are not

338   essential *in hospite*. However, this appears to not be the case in coral endosymbiosis,

339   given that all sequenced Symbiodiniaceae genomes are of approximately one gigabase

340   in size (Aranda et al., 2016; Lin et al., 2015; Liu et al., 2018; Shoguchi et al., 2013), nor

341   should it be expected, given that the coral endosymbiont must maintain the full

342   complement of genes for free-living persistence, as the majority of corals uptake their

343   endosymbionts from the free-living environment (Baird et al., 2009; Richmond and

344   Hunter, 1990). Further, Symbiodiniaceae have been found to exist in a free-living state

345   in numerous environments, including sediments and other benthic substrates, as

346   epiphytes, and in the water column (Granados-Cifuentes et al., 2015; Littman et al.,

347   2008; Takabayashi et al., 2012).

348   Despite this lack of genome reduction in Symbiodiniaceae, we identified a

349   significant downregulation of gene expression *in hospite* compared to free-living *D.*

350   *trenchii* at both temperatures. Free-living Symbiodiniaceae appear to require to a larger

351   transcriptional repertoire to persist in an extracellular environment, for functions

352   presumably including motility and coping with fluctuations experienced outside of the

353   confines of a host cell. This substantial downregulation of transcripts *in hospite* is

354   associated with enrichment of transcripts associated with heterochromatin organization

355   histone H3-K9 methylation (Fig. S2). The hypermethylated state of cultured, free-living

356   Symbiodinaceae was demonstrated by ten Lohuis and Miller (ten Lohuis and Miller,

357   1998), but comparisons to the *in hospite* condition have not been performed. Our results

15

358   suggest that chromatin remodeling may play an important role in the switch between the

359   free-living state and endosymbiosis, contributing to the substantial downregulation

360   associated with the symbiotic life phase. We consider this resulting transcriptome

361   reduction analogous to the genome reduction observed in numerous obligate symbiotic

362   systems.

The potential for sex in free-living Symbiodiniaceae

364   In many species, sex and reproduction are inextricably linked, but for some, sex

365   represents a special occasion. For instance, consider a member of a taxon sister to the

366   dinoflagellates, the apicomplexan *Plasmodium falciparum*. This malaria-causing

367   parasite only engages in sexual reproduction within its mosquito host (Kooij and

368   Matuschewski, 2007; Talman et al., 2004). Be it frequent or rare, the function of sex,

369   despite its apparent ubiquity, is not a settled case. One hypothesis regarding the

370   evolution of sex is that recombination mediated by sexual reproduction arose as a

371   mechanism to repair DNA damage in an individual (Bernstein et al., 1985). A competing

372   hypothesis holds that the advantage of meiotic recombination resides in the genetic

373   diversity afforded to offspring (Burt, 2000; Otto, 2009).

374   The role of sexual reproduction in the Symbiodiniaceae life cycle remains an

375   open question. A broad survey of Symbiodiniaceae by Santos and Coffroth (Santos and

376   Coffroth, 2003) concluded that Symbiodiniaceae are diploid in the vegetative life phase,

377   both in cultured and *in hospite* cells. However, apparent tetrads have long been

378   reported in cultured Symbiodiniaceae (Freudenthal, 1962), but it remains unknown

379   whether these tetrad-like arrangements represent meiotic events or simply two rounds

380   of mitosis. Symbiodiniaceae meiosis has yet to be demonstrated in an experimental

381   setting, but others have identified population genetic evidence of recombination (Baillie

382   et al., 2000; LaJeunesse, 2001). Further, Symbiodinaceae genomes possess a virtually

383   complete gene set for meiosis (Liu et al., 2018), suggesting that they have the potential

384   for sexual reproduction.

385   We posit that the free-living phase of life in Symbiodinacaea may provide the

386   opportunity for sex and recombination in the free-living state. In comparisons at 28°C,

387   several meiosis-related transcripts are upregulated in the free-living state in comparison

388   to the *in hospite* condition (*MSH6, RAD54*, *MEI2-like 2*, *MEI2-like 3*, and *MEI2-like 5*).

389   Our work also identifies a subset of these meiotic transcripts (three *MEI2-like 5*

390   transcripts*)* in the core heat stress response of *D. trenchii* that is shared by both *in*

391   *hospite* and free-living states. While Levin et al. (2016) also detected an upregulation of

392   meiosis-related genes under conditions of thermal stress in culture conditions, our work

393   adds a nuanced understanding of alterations in meiosis-related gene expression

394   between free-living and *in hospite D. trenchii.*

395   Recombination through sexual reproduction may be critical to the maintenance of

396   Symbiodiniaceae genomes. Muller's Ratchet dictates that asexual reproduction without

397   other forms of recombination has the potential for the accumulation of deleterious

398   mutations over generations (Felsenstein, 1974; Muller, 1964, 1932). This effect has

399   support from RNA viruses lacking recombination (Chao, 1997) and may be one of the

400   driving forces behind genome reduction in obligate endosymbionts (Andersson and

401   Kurland, 1998), but obligate symbionts may have other mechanisms to avert genomic

402   meltdown. Selection at the level of the holobiont has been suggested as one

403   mechanism of endosymbiont genome maintenance (Rispe and Moran, 2000), with

404   genomic degradation and losses observed likely to be neutral or nearly neutral

405   (Pettersson and Berg, 2007). We posit that recombination in the free-living phase of

406   Symbiodiniaceae may be instrumental in genomic maintenance of functions necessary

407   for the free-living state.

408   **Evasion of host immunity by symbiont-derived factors**

409   In order to maintain a stable endosymbiotic existence, members of the family

410   Symbiodiniaceae must evade the host immune system. A considerable number of

411   studies have shown that Symbiodiniaceae suppress and/or circumvent host immunity in

412   order to colonize and persist *in hospite*; multiple mechanisms of circumvention appear

413   to occur, including the suppression of apoptosis (Matthews et al., 2017; Rodriguez-

414   Lanetty et al., 2006; Tchernov et al., 2011) as well as the manipulation of markers of

415   endosome age (Chen et al., 2005, 2004, 2003). More recent work has identified

416   endosymbiont miRNAs which target host transcripts involved in immunity (Baumgarten

417   et al., 2018, 2013). We identified numerous transcripts involved in the suppression of

418   innate immunity and anti-inflammatory pathways, including a putative NRCL3 ortholog

419   and NF-κB inhibitor, which are upregulated in the symbiotic state. However, in order for

420   this to plausibly occur, the symbiont must be able transmit these signals to the host.

421   Based on transcriptome evidence, we postulate mechanisms for this below.

422   Apicomplexans, including parasites in the genus *Plasmodium,* possess

423   structures that form an apical complex which functions in host invasion and secretes

424   effectors into the host (reviewed by (Kemp et al., 2013). Cellular machinery in

425   Symbiodinaceae involved in the delivery of immune-suppressing factors to the host

426   remain unexplored, but this work identifies several abundant transcripts with homology

18

427   to components of the apicomplexan apical complex. One component of the apical

428   complex are micronemes, bar-like organelles which release micronemal proteins critical

429   for host cell recognition and attachment, linking parasite and host cell receptors (Brecht

430   et al., 2001; Carruthers and Tomley, 2008; Friedrich et al., 2010; Soldati et al., 2001)

431   and further are critical for the trafficking and storage of ligands for host-cell receptors

432   (Soldati et al., 2001).

433   *D. trenchii* possess numerous transcripts with homology to proteins associated

434   with the apicomplexan apical complex, including three apical complex lysine

435   methyltransferase transcripts (TRINITY_DN22464_c0_g1_i2,

436   TRINITY_DN12687_c0_g1_i1, and TRINITY_DN59290_c0_g1_i1) and AGC/AKT

437   protein kinase transcripts (TRINITY_DN23213_c0_g1_i1 and

438   TRINITY_DN55685_c0_g1_i1), and three putative microneme proteins

439   (TRINITY_DN25568_c0_g1_i1, TRINITY_DN48019_c0_g1_i1, and

440   TRINITY_DN29950_c0_g1_i3). While the majority of these transcripts are not

441   differentially expressed, two are highly upregulated *in hospite*. One of these transcripts

442   (TRINITY_DN29950_c0_g1_i3) is a putative ortholog of a *Toxoplasma* microneme

443   protein 4 (MIC4). In its role in infection, the *Toxoplasma* MIC4 is thought to contribute to

444   parasite adhesion by acting as a bridge between receptors on the parasite and the host

445   cell (Brecht et al., 2001). Another transcript upregulated *in hospite* with homology to

446   apicomplexan invasion machinery is a cGMP-dependent protein kinase

447   (TRINITY_DN29950_c0_g1_i3) which Collins et al. (Collins et al., 2013) show is

448   required for the release of micronemes in *Plasmodium*. Taken together, these

449   transcripts suggest the possibility of components of an apicomplexan-like apical

19

450   complex involved in the maintenance of intracellular symbiosis by *D. trenchii*, and

451   potentially the delivery of symbiont-derived factors which suppress the host immune

452   response to allow stable endosymbiosis.

Enhanced ammonium and ABC transporter activity *in hospite*

454   The controlled exchange of materials between the symbiont and host is of critical

455   importance for the persistence of both partners (Behie and Bidochka, 2014; Moya et al.,

456   2008). Our study identified transporters active in the symbiotic state for both ammonium

457   transport and assimilation, as well as a diverse group of ABC transporters which may be

458   involved in the movement of numerous as-yet unidentified substrates into and out the

459   symbiont.

460   The acquisition of inorganic nitrogen is of critical importance to photosynthetic

461   endosymbionts. Pernice et al. (Pernice et al., 2012) demonstrated that *in hospite*

462   dinoflagellates fix 14 to 23 times more nitrogen than coral host cells in ammonium-

463   enriched water. In the *in hospite* state, we identify the upregulation of an ammonium

464   transporter transcript as well as two glutamine synthetase transcripts. This is congruent

465   with the longstanding support for glutamine synthetase activity as the mechanism by

466   which Symbiodinacaea assimilate ammonium from seawater and re-assimilate waste

467   ammonium from the cnidarian host (Anderson and Burris, 1987).

468   In the *in hospite* state, five transcripts annotated as ABC transporters are

469   upregulated in comparison to the free-living state at 28°C (Table S5). While numerous

470   host ABC transporters are upregulated in the proteomes of symbiotic *Exaiptasia pallida*

471   by Matthews et al. (2017), with earlier work by Peng et al. (2010) identifying an ABC

472   transporter associated with the symbiosome, this represents the first functional

20

473   evidence *in hospite* Symbiodiniaceae transporter activity in a cnidarian. ABC

474   transporters comprise a family of proteins responsible for the transport of diverse

475   substrates, including ions, nutrients, amino acids, peptides, proteins, lipids, metals,

476   lipids, oligonucleotides, and sugars (Locher, 2016; Wilkens, 2015).

477   **Conclusion**

478   In summary, our results demonstrate that symbiotic state has major impacts on

479   Symbiodiniaceae gene expression, both in steady state symbiosis and under conditions

480   of acute thermal stress. While prior work has found physiological differences between *in*

481   *hospite* and free-living Symbiodiniaceae (e.g. Banaszak and Trench, 1995; Bhagooli et

482   al., 2008), effect of the intracellular habitat on the transcriptome has not previously been

483   appreciated. The *in hospite* response to thermal stress differs dramatically from that of

484   free-living *D. trenchii*, with the transcriptome of *in hospite* endosymbionts hallmarked by

485   higher differential gene expression activity overall and enriched for mRNA transport

486   activity as well as a specialized cell adhesion process. While we identify a core heat

487   stress response shared between free-living and *in hospite D. trenchii*, this represents

488   only a minority of transcriptional activity. Our findings also reveal the divergent

489   processes at work in free-living and *in hospite* cells under non-stress conditions, with

490   free-living *D. trenchii* exhibiting evidence suggestive of sexual reproduction and *in*

491   *hospite* cells displaying reduced differential expression in a process we term

492   transcriptome reduction, as well as putative host evasion activity. We posit that the

493   observed transcriptomic reduction of non-essential genes *in hospite* may be an

494   alternative adaptive strategy to genome reduction for endosymbionts that must also

495   maintain the capacity for a free-living life phase. We intend for this to serves as the

496   basis for future gene editing efforts to understand the genetic basis of symbiosis and

497   dysbiosis, with the ultimate aim of engineering of stress-tolerant coral endosymbionts.

498   These efforts will for provide additional options in future reef protection and restoration

499   efforts desperately needed for the persistence of coral reefs into the 21st century.

500

Materials and Methods

502   Aposymbiotic *Exaiptasia pallida* (strain CC7) were inoculated with *D. trenchii*

503   (strain CCMP2556) and maintained with feeding of *Artemia franciscana* twice weekly for

504   12 months. Free-living *D. trenchii* were cultured in Prov50 (Smith and Chanley, 1975)

505   medium and maintained in log phase via regular passage. To identify thermal

506   treatments that elicited an acute heat stress response, *Durusdinium trenchii* (strain

507   CCMP2556) cultures were exposed to thermal stress and assessed with PAM

508   fluorometry (Fig. S1). Based upon the observed rapid decline in Fv/Fm at 34 °C in

509   contrast to the maintained photosynthetic efficiency at 28 °C (Fig. S1), these treatments

510   were selected and implemented for comparisons following 6 hours at the target

511   temperatures. Symbiotic anemones and free-living *D. trenchii* cultures were held at

512   28°C under light intensity levels of 80 µE (12:12 light:dark cycle) and ramped up to the

513   34°C challenge at a rate of 2°C per day for thermal stress treatments, with increases of

514   temperature performed at the beginning of the photoperiod. Free-living (cultured) *D.*

515   *trenchii* and *in hospite D. trenchii* were frozen in liquid nitrogen mid-photoperiod for

516   sampling. Heat stress treatments were exposed to 34°C for a total of six hours. The

517   experiment was replicated temporally (n=3-4). Total RNA was extracted from

518   Symbiodiniaceae cells, with *in hospite* samples depleted of cnidarian host material prior

519   to extraction using a novel endosymbiont enrichment method (See Supplement 1 for

520   detailed methods). Stranded RNAseq libraries were prepared from poly(A) selected

521   RNA with the NEBNext Ultra RNA Library Prep Kit (NEB, Cambridge, MA) and

522   sequenced across two Illumina HiSeq lanes. A reference transcriptome was assembled

523   and filtered to remove host, other non-Symbiodiniaceae transcripts, and ribosomal RNA

524   transcripts. Principal component analysis was conducted using the prcomp function

525   from the stats package within R and statistical inference of significant transcripts driving

526   the principal components was conducting using the jackstraw package in R. The

527   resulting transcriptome was annotated using Trinotate (https://trinotate.github.io/) with

528   BLASTX and BLASTP searches performed against the SwissProt and Uniref90

529   databases using DIAMOND, an accelerated sequence aligner comparable to NCBI

530   BLAST+ (Buchfink et al., 2015). Following Trinotate, we employed the structural protein

531   homology detection program HH-Pred and the PDB70 database to identify remote

532   homologs in all remaining un-annotated transcripts using a strict cut-off of 80%

533   probability. Annotation was further supplemented by using Blast2GO (Conesa et al.,

534   2005) in combination with BLASTX searches against the non-redundant NCBI protein

535   database with DIAMOND and Interproscan under default settings. Gene ontology terms

536   acquired for each transcript during the annotation process from Trinotate, HHPred

537   (Söding et al., 2005), and Blast2GO were merged and redundant terms resulting from

538   the integration of the three annotation tools were removed prior to downstream

539   analyses. Following transcript quantification with Salmon (Patro et al., 2017), differential

540   gene expression analysis was performed in edgeR (Robinson et al., 2010) using a

541   generalized linear model to determine the effects of temperature and symbiotic state as

23

542   well as the interaction between the two on changes in transcript expression.

543   Differentially expressed transcripts were subject to gene ontology (GO) enrichment

544   analyses within the R package topGO (Alexa and Rahnenführer, 2016). GO results for

545   comparisons were visualized using REVIGO (Supek et al., 2011). Methods are
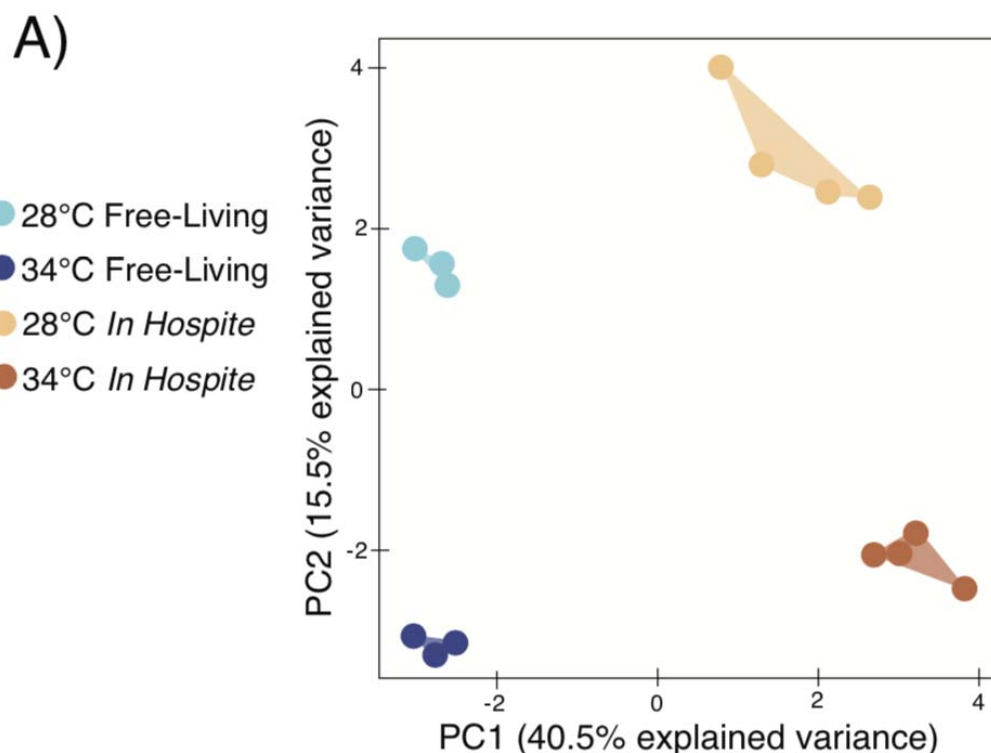
546   described in detail in Supplement 1.

547

548   **References**

549

550
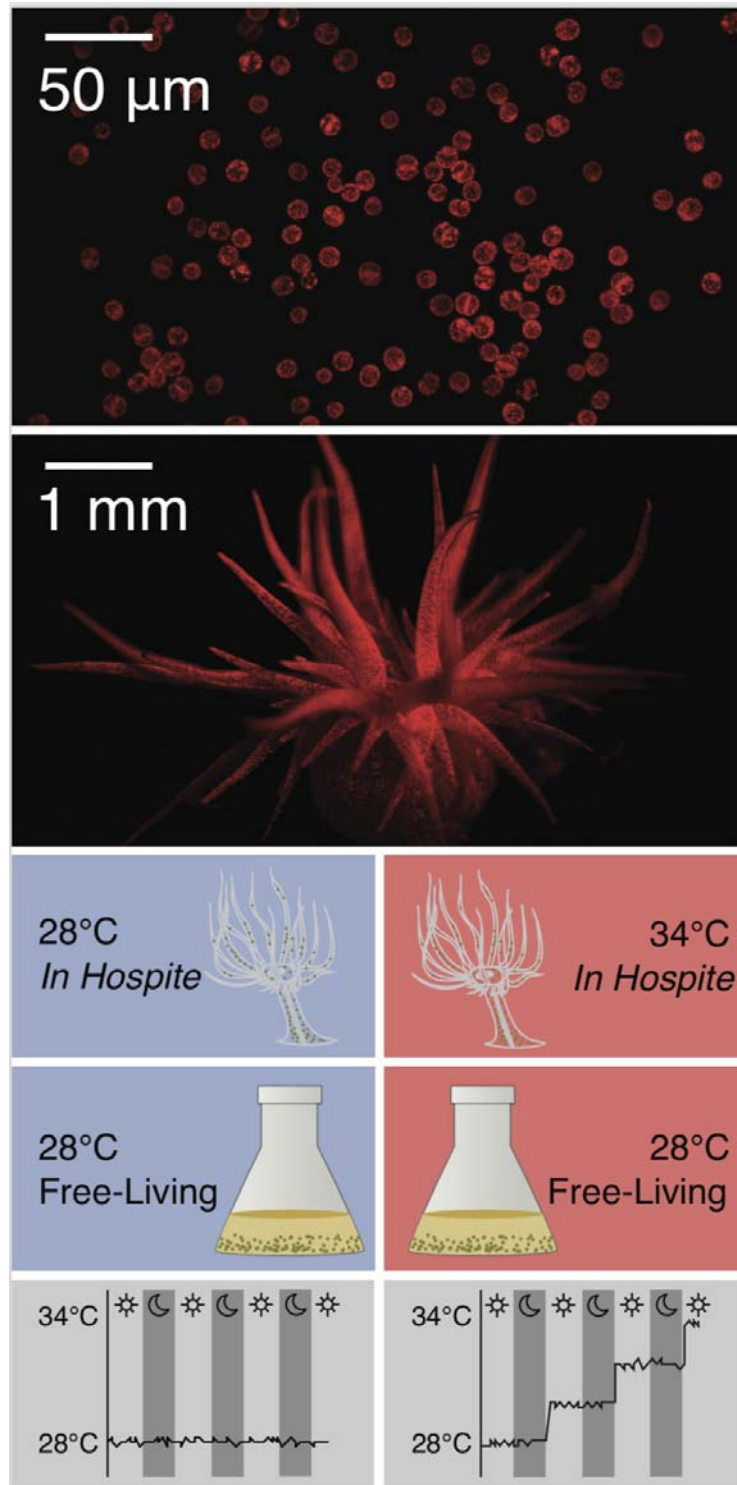
Figure 1: *Durusdinium trenchii in free-living culture state (top) and in hospite in E. pallida (second panel). Schematic of experimental treatments (lower panels) comparing symbiotic state and thermal stress, with temperature and light profiles.*

25

555

556

557 **Figure 2.** *A) Principal component analysis depicting the ordination of biological*

558 *replicates by all analyzed transcripts. (B) Summary of the number of transcripts driving*

559 *PC1 and PC2, the number of transcripts DE according to edgeR, and the number of*

560 *transcripts that were both DE and significant drivers of PC1 and PC2.*

561

562
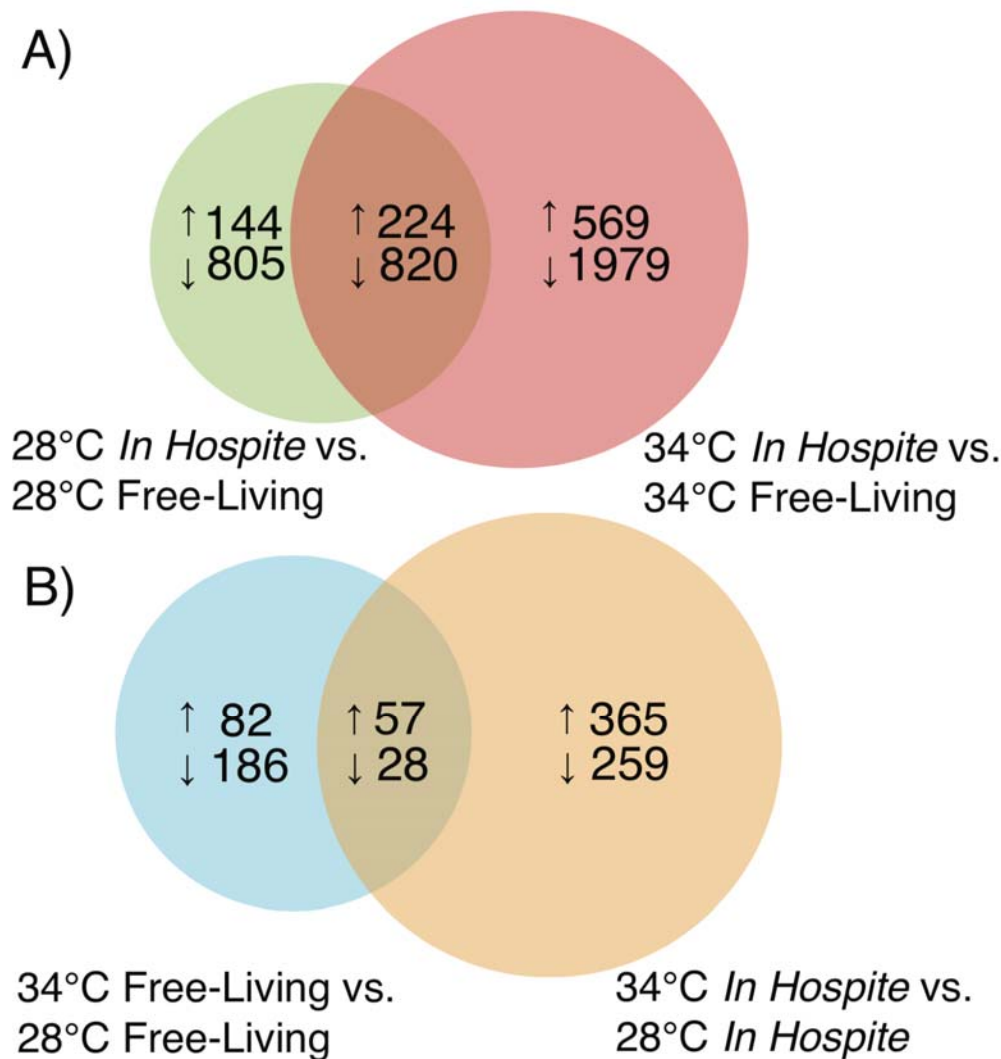
Figure 3. *Venn diagrams of the number of differentially expressed transcripts by*

pairwise comparison (FDR-corrected p < 0.01, greater than 2-fold difference). A)

Contrasts transcriptional changes between in hospite and free-living transcripts at 28°C

and 34°C. B) Comparison of transcripts differentially expressed in the free-living and in

hospite condition, with the core heat stress response represented by the overlapping

region.

570
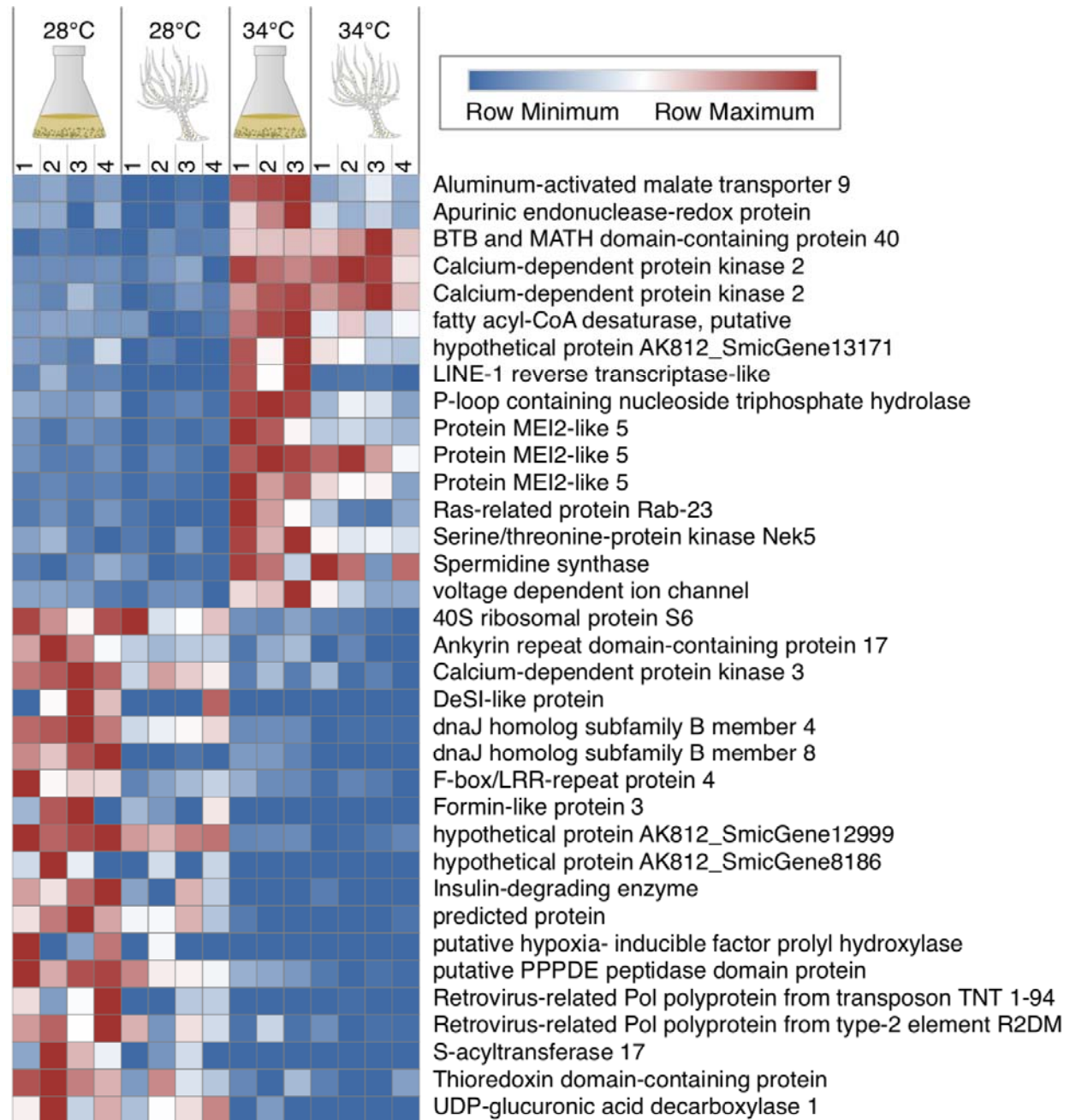
Figure 4. *Core heat stress response transcripts. The heatmap reflects annotated*

transcripts differentially expressed in both in hospite and free-living thermal stress

conditions. (Unannotated transcripts omitted.)

571

572

573

574

575
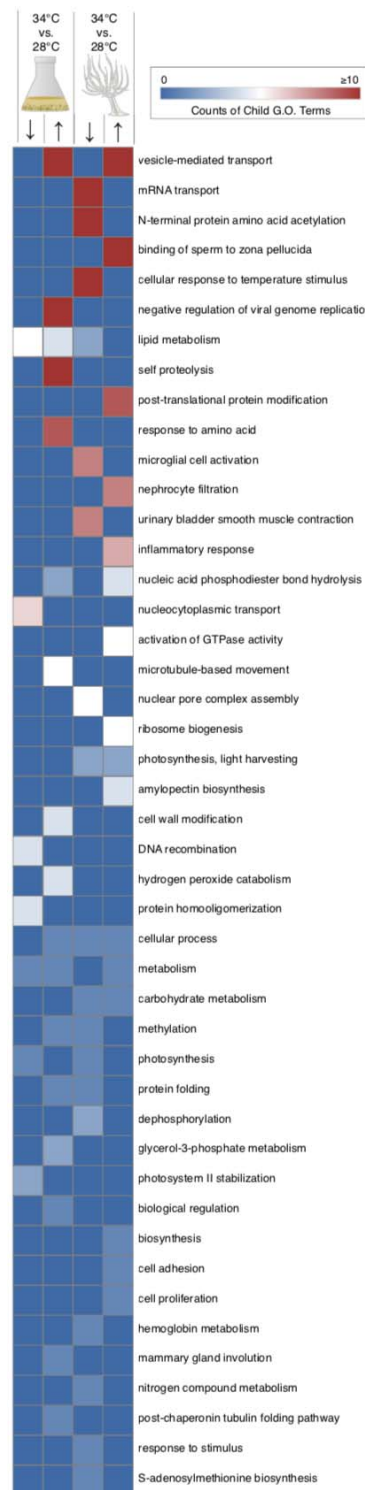
Figure 5. *Counts of GO terms enriched exclusively in the free-living and in hospite heat stress response. (Terms associated with transcripts differentially expressed in both in hospite and free-living conditions were excluded from this enrichment analysis).*

29

Figure 6. *Counts of GO terms associated with up- and downregulated transcripts across all comparisons. Parent GO terms are listed for all categories with a minimum sum of two daughter terms across all comparisons.*

Supplement 1

Supplemental Materials and Methods

Experimental Overview

Briefly, the experimental design compares D. trenchii in the free-living state (culture) and in hospite in an Exaiptasia host under two different temperature regimens, a steady-state culture temperature of 28°C and a thermal stress of 34°C, both under light intensity levels of 80 µE. Four biological replicates of each condition were implemented, with replication performed in time.

Exaiptasia symbiont manipulation and Symbiodinacaea culture

Aposymbiotic Exaiptasia were produced through repeated cold treatment (8 hours at 4°C, repeated three times over the course of one week) followed by DCMU treatment (50 uM) performed for 6 hours with 1000 µmol m−2 s−1 light intensity, repeated twice weekly for 3 weeks. Absence of dinoflagellates was confirmed with fluorescent microscopy. D. trenchii strain CCMP2556 was obtained from the National Center for Marine Algae and Microbiota (East Boothbay, Maine) and cultured in Prov50 media under a 12:12 light cycle. Log phase cultures were used for all experiments. Aposymbiotic anemones were challenged with 100,000 log phase Durusdinium trenchii cells combined with freshly hatched Artemia franciscana in a total volume of 10 ml of sterile seawater, with water replaced after 12 hours . Infection was confirmed by fluorescent microscopy, followed by PCR and sequencing of 23S. Anemones hosting D. trenchii were grown for one year prior to experimental manipulation with light levels at

31

606   *approximately 80 µmol m−2 s−1. Anemones were fed freshly hatched Artemia twice*

607   *weekly.*

608   **Symbiosis state comparison and thermal challenge**

609   *To inform the design of this experiment, maximum quantum yield in cultured D.*

610   *trenchii was assessed through time, at temperatures from 28 to 36° C (n=3) using a*

611   *PAM fluorometer (Walz, Germany). We found that the rapid decline in maximum*

612   *quantum yield began at 34°C at 2 hours of thermal stress. In an 8 hour timespan, we did*

613   *not find significant decline at the lower thermal treatments.*

614   *Anemones and cultures were maintained at 28°C with 80 µmol m−2 s−1*

615   *irradiance and ramped up to the 34° C challenge at a rate of 2°C per day for thermal*

616   *stress treatments. Mid-photoperiod (6 hours into light phase of the diel cycle), samples*

617   *were frozen for subsequent RNA extraction. Log phase D. trenchii cultures were used*

618   *for all experiments. Replicates were performed in time, with one replicate of each*

619   *treatment included in each trial. A total of four biological replicates were collected for*

620   *each treatment.*

621   **Symbiodinacaea RNA Extraction Enrichment Protocol**

622   *Anemones were frozen in minimal seawater in 2 ml cryotubes in liquid nitrogen*

623   *and stored at -80°C till extraction. For enrichment of Symbiodiniaceae from anemone*

624   *extractions, 500 ul of Buffer RLT with 0.1% 2-mercaptoethanol (Qiagen) was added to*

625   *each tube and manually flicked till frozen tissue was dislodged and decanted into 1.5 ml*

626   *centrifuge tube. Tissue was gently homogenized with a plastic pestle and vortexed at*

627   *maximum speed for 1 minute. Homogenate was centrifuged at 10,000 g for 3 min. Clear*

628   *supernatant was carefully removed and discarded, leaving the symbiont pellet intact.*

32

629   *This pellet was resuspended in 1.4 ml of Buffer RLT and vortexed till the mixture was*

630   *homogenous. This suspension was centrifuged at 3,000 g for 3 min. Clear supernatant*

631   *was discarded, and an additional 1.4 ml of Buffer RLT was added vortexed till*

632   *homogenous. This was centrifuged at 3,000 g for 3 minutes and clear supernatant was*

633   *discarded prior to resuspension in 600 ul Buffer RLT. Contents were transferred to a*

634   *screw top 2.0 ml tube and bead beat for 1 min at 6 m/s with glass beads. Homogenate*

635   *was processed with the Qiagen RNeasy Kit as per manufacturer instructions, with an*

636   *additional RPE Buffer wash prior to elution of total RNA. Symbiodiniaceae were snap*

637   *frozen in liquid nitrogen and extracted alongside anemone tissue, implementing an*

638   *identical washing scheme to eliminate any extraction-based bias.*

639   ***Library Construction and Sequencing***

640   *Following poly(A) selection from total RNA, RNAseq libraries were constructed*

641   *from mRNA using the NEBNext Ultra Directional RNA Library Prep Kit (NEB). A total of*

642   *16 libraries were sequenced on two Illumina HiSeq lanes, using v4 150 base pair*

643   *paired-end chemistry (Illumina). The indexed samples were pooled across both lanes to*

644   *eliminate lane effects. Raw data have been archived on the SRA and is available under*

645   *NCBI TSA BioProject PRJNA508937.*

646   ***De novo transcriptome assembly***

647   *Quality of the resulting raw reads were assessed via FastQC and low-quality*

648   *reads were removed and/or trimmed with Trimmomatic (Bolger et al., 2014) with a*

649   *minimum read length threshold of 50 bp. Trimmed reads that aligned concordantly*

650   *against the human and Exaiptasia pallida genomes using the HISAT2 (Kim et al., 2015)*

651   *program to remove any contaminating eukaryotic reads. Remaining reads were then*

652   *filtered using all bacterial, archaeal, and viral genomes present in RefSeq (as of Sep. 8,*

653   *2017) using Kraken, an ultra-fast taxonomic sequence classification program (Wood*

654   *and Salzberg, 2014). The 526,545,945 remaining PE reads were then assembled with*

655   *Trinity v2.4.2 (Grabherr et al., 2011) with a minimum contig length of 200 bp.*

656   *Redundant contigs were removed using uCLUST (Edgar, 2010) at an identity*

657   *threshold of 100%. Removal of eukaryotic contaminants via Hisat2 and prokaryotic*

658   *contigs via Kraken (Wood and Salzberg, 2014) was repeated once more on the*

659   *transcriptome assembly to remove any lingering contamination that could not be*

660   *identified from the raw reads. Ribosomal RNA contamination was identified and*

661   *removed by aligning transcriptome contigs against all of the SILVA rRNA databases*

662   *(Quast et al., 2012) with Bowtie2 (Langmead and Salzberg, 2012) resulting in a final*

663   *assembly of 85,130 contigs. Assembly statistics were calculated using Transrate*

664   *(Smith-Unna et al., 2016) (Supplementary Table 1).*

665   *For annotation, the assembly was searched against the NR protein database*

666   *using DIAMOND, a fast search algorithm that employs double-indexing and spaced*

667   *seeds of various weights and shape to make it ~20,000x faster than BLASTX with*

668   *comparable level of sensitivity and accuracy (Buchfink et al., 2015). These results were*

669   *input into with Trinotate using BLASTP and BLASTX searches against the SwissProt*

670   *and Uniref90 databases with an e-value cutoff of $< 1 \times 10^{-5}$. Open reading frames*

671   *(ORFs) were predicted using Transdecoder under the default settings. Gene ontology*

672   *classifications were extracted from search results against the SwissProt database. The*

673   *searches were conducted using DIAMOND, a fast search algorithm that employs*

674   *double-indexing and spaced seeds of various weights and shape to make it ~20,000x*

34

675   *faster than BLAST with a similar sensitivity and accuracy (Buchfink et al., 2015).*

676   *Additional annotation was performed using Blast2GO (Conesa et al., 2005), with*

677   *redundant GO terms removed with a custom script.*

678   *Quality-controlled reads were mapped back to the final assembly using Salmon*

679   *at an average mapping rate of 88% and 30.1 million reads per sample. Mapping results*

680   *were imported into R for differential gene expression analysis with the edgeR package*

681   *(Robinson et al., 2010). Low-count transcripts that across all samples with a mapping*

682   *rate of < 10 reads were removed prior to count normalization within R. Differential gene*

683   *expression anlysis was then performed in edgeR using a generalized linear model to*

684   *determine the effects of temperature and symbiotic state as well as the interaction*

685   *between the two on changes in gene expression. Four pairwise comparisons were then*

686   *conducted using the GLM: (1) free-living at 28 °C vs. free-living at 34 °C (2) symbiotic at*

687   *28°C vs. symbiotic at 34 °C (3) free-living at 28 °C vs. symbiotic at 28 °C and (4) free-*

688   *living at 34 °C and symbiotic at 34 °C. An additional comparison with the GLM was done*

689   *using the formula ((symbiotic at 34 °C vs. free-living at 34 °C) - (free-living at 28 °C vs.*

690   *symbiotic at 28 °C)) to determine genes that were differentially expressed in response*

691   *to symbiosis but responded differently to temperature. Results from each of the five*

692   *comparisons in edgeR were then used for gene ontology (GO) enrichment analyses*

693   *within the R package topGO. GO results for the different comparisons were summarized*

694   *and viewed using the web-based REVIGO program (Supek et al., 2011).*

695

696   *Supplement 1 (Supporting Figures and Tables)*

697

698
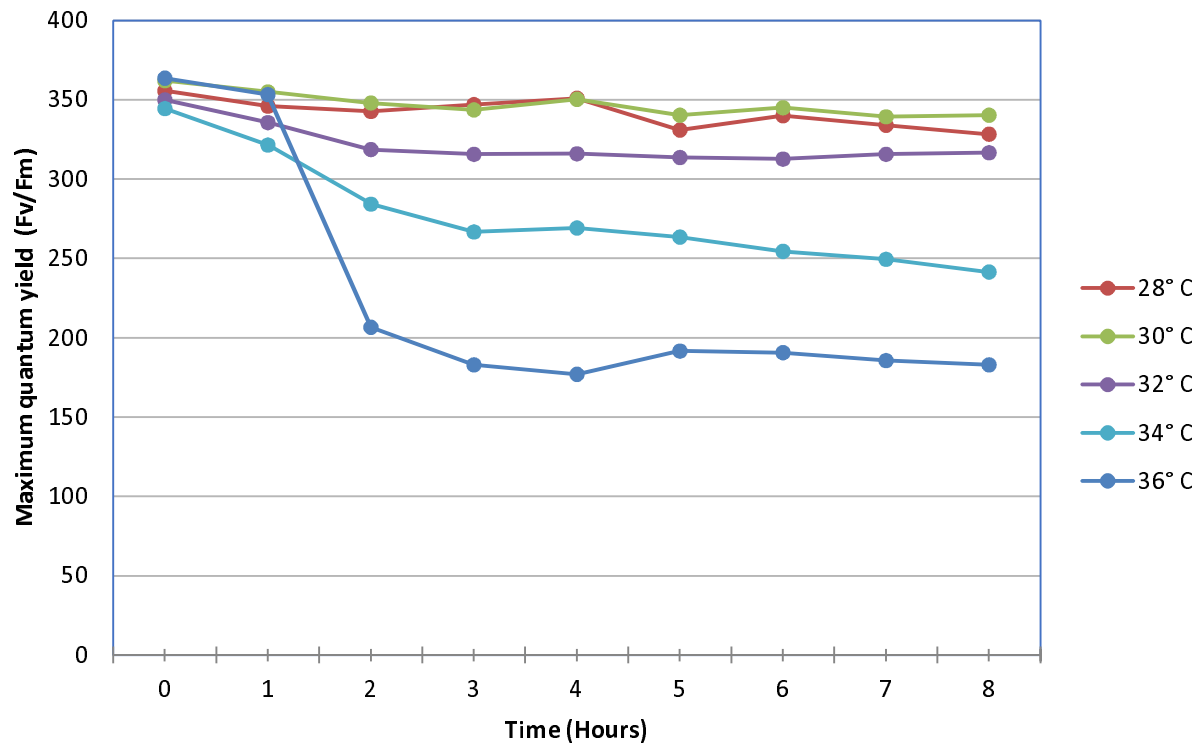
699   **Supplementary Figure 1.** *Maximum quantum yield of D. trenchii cultures assessed via*

700   *PAM fluorometry throughout a thermal stress timecourse.*

701

702

36

703
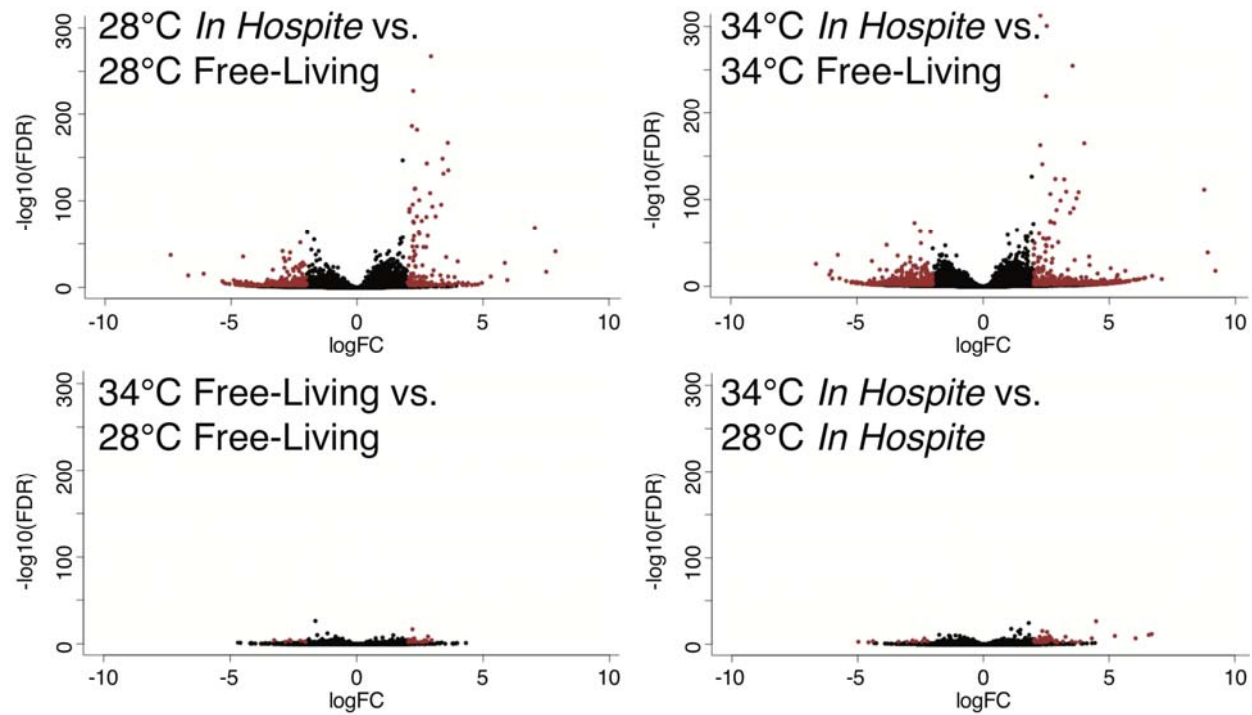
Supplementary Figure 2. *Volcano plots of all transcripts; transcripts with FDR*

corrected p-value < 0.01 and greater than log_2 2-fold difference are indicated in red.
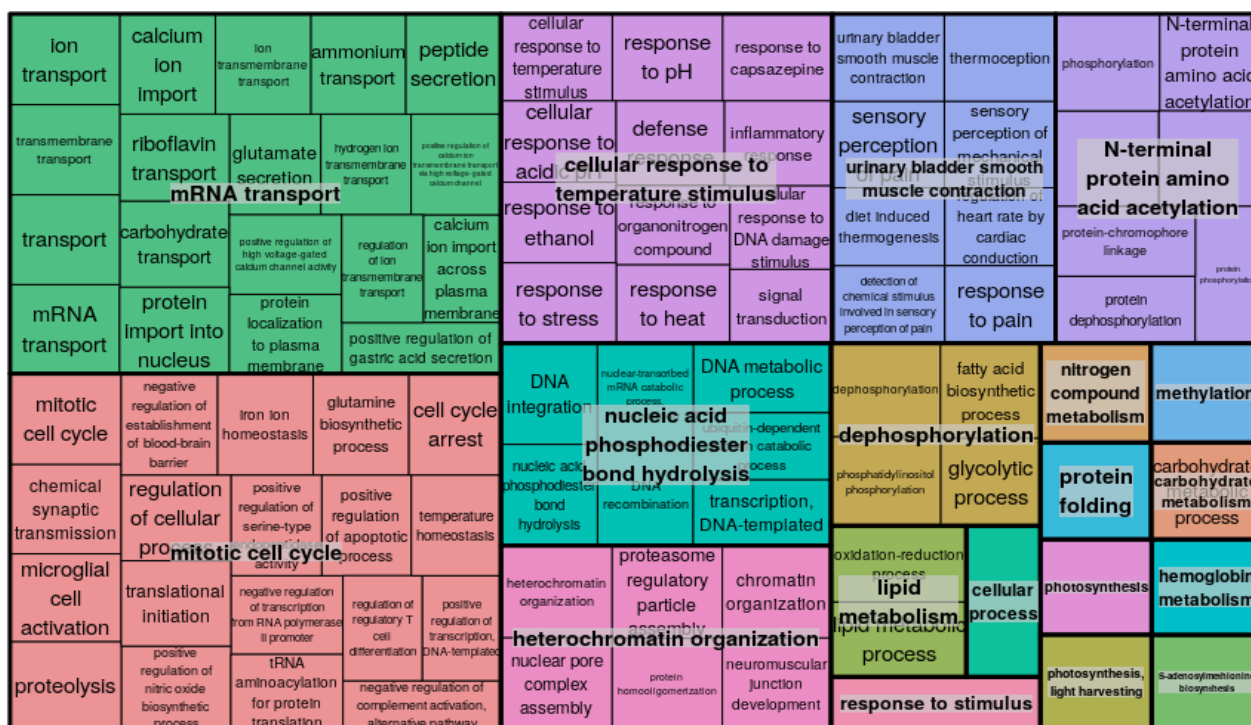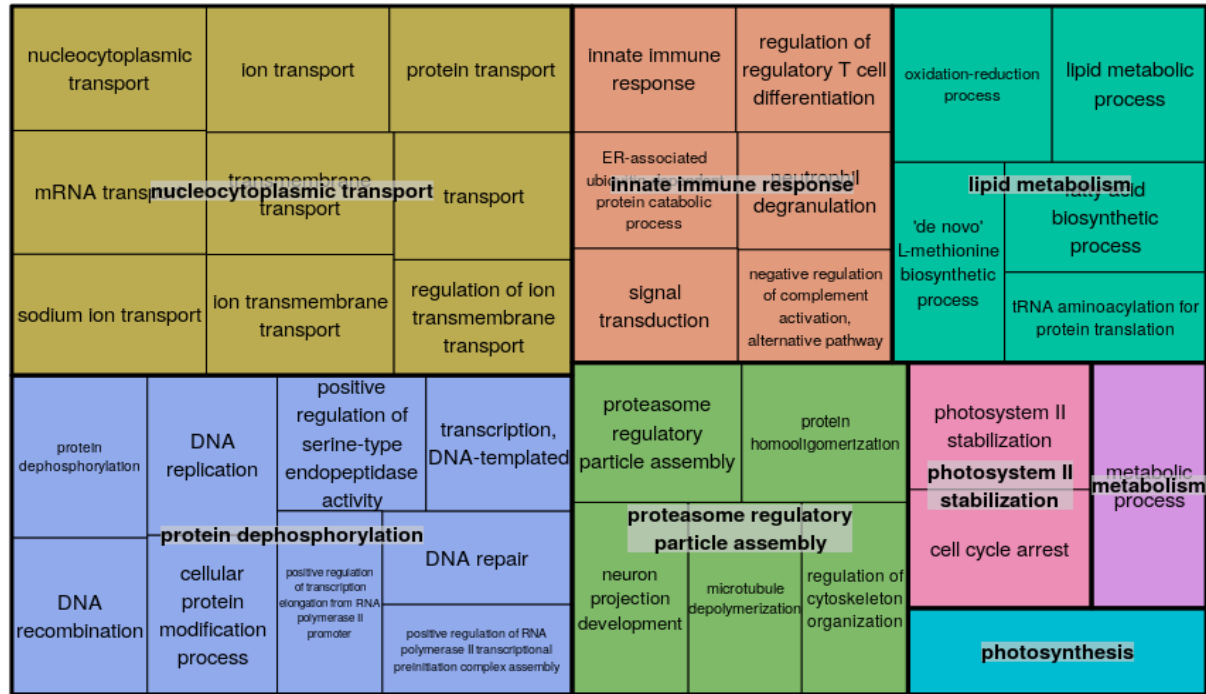
704

705

706

707

708
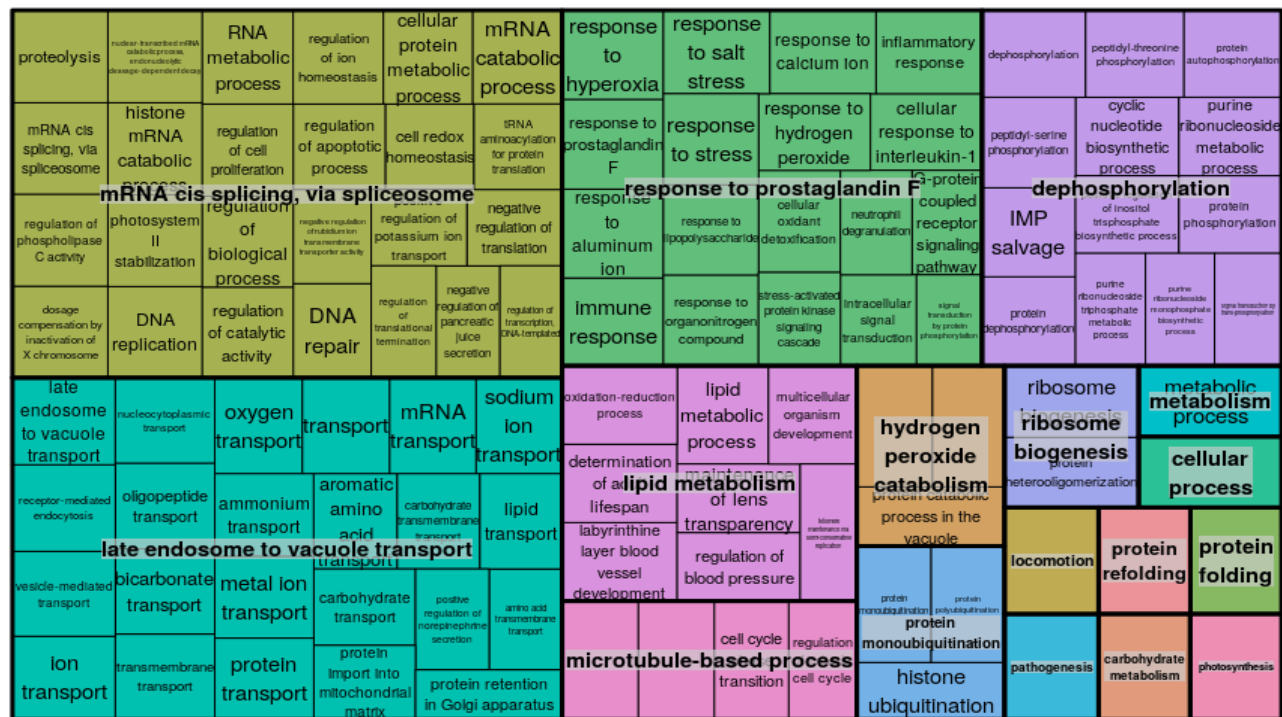
Supplementary Figure 3. *REVIGO tree diagram summary of the GO terms associated*

with transcripts up-regulated in response to symbiosis compared to free-living D.

trenchii at 28 °C.

712

713

714

715
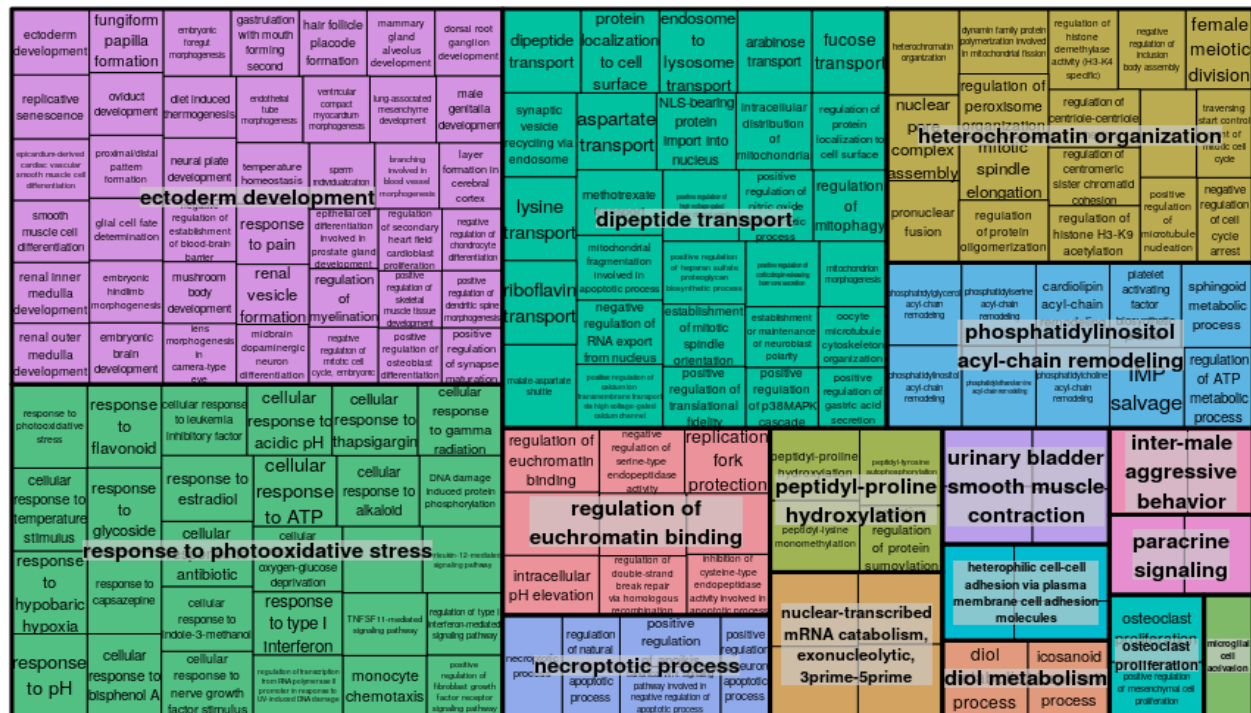
716 **Supplementary Figure 4.** *REVIGO tree diagram summary of the GO terms associated*

717 *with transcripts down-regulated in response to symbiosis compared to free-living D.*

718 *trenchii at 28 °C.*

719

720

721

722

723 **Supplementary Figure 5.** *REVIGO tree diagram summary of the GO terms associated*

724 *with transcripts up-regulated in response to symbiosis compared to free-living D.*

725 *trenchii at 34 °C.*

726

727

728
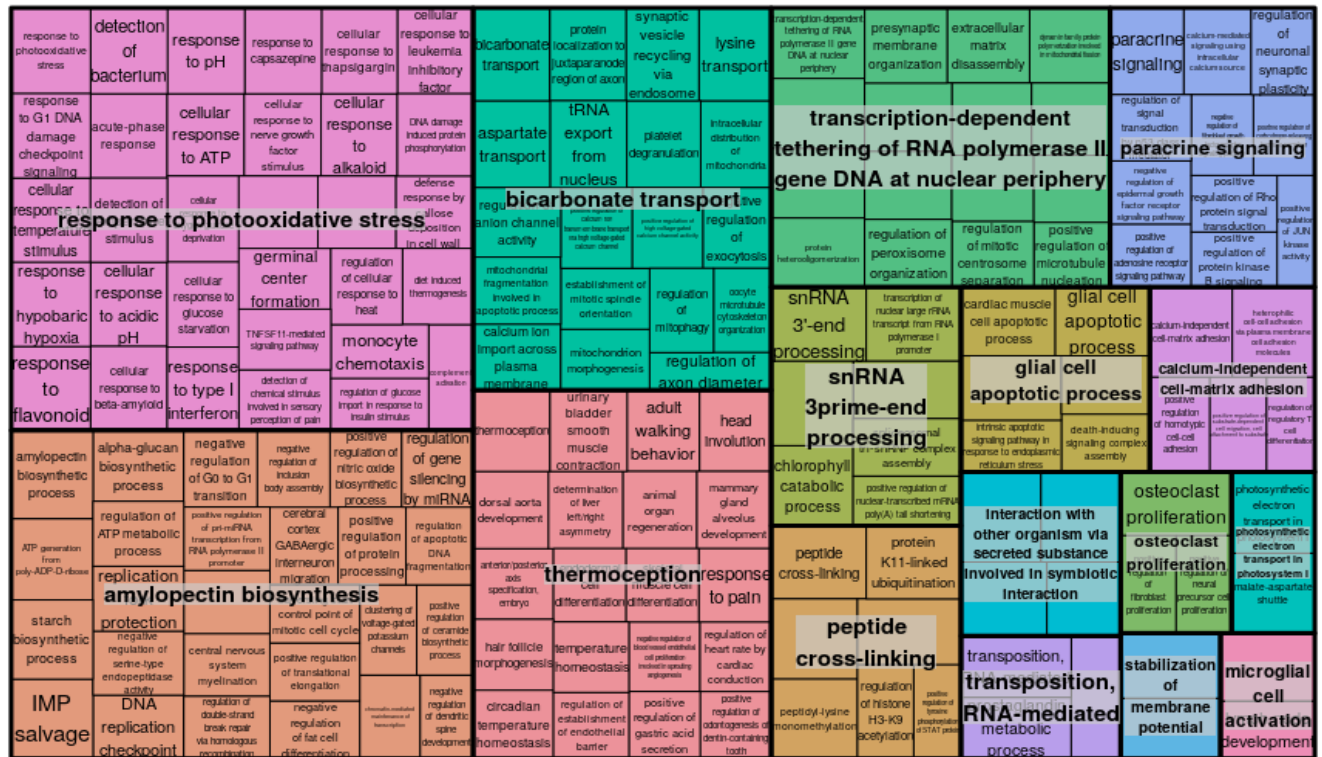
Supplementary Figure 6. REVIGO tree diagram summary of the GO terms associated with transcripts down-regulated in response to symbiosis compared to free-living D. trenchii at 34 °C.
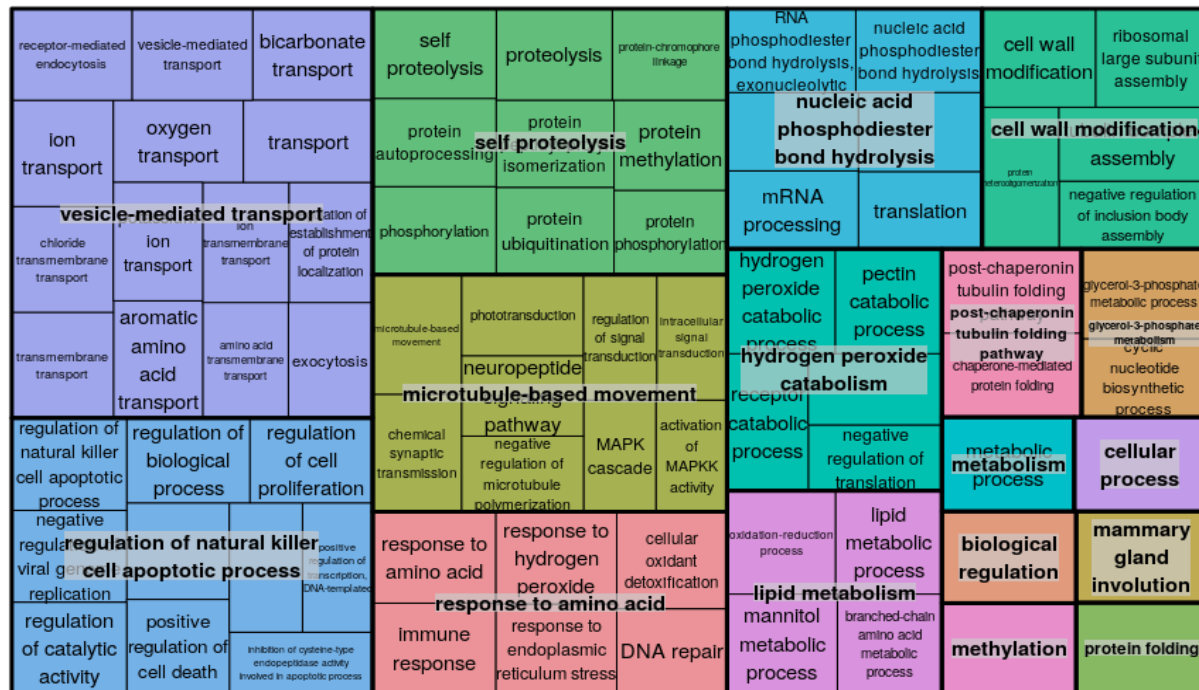
732

Supplementary Figure 7. *REVIGO tree diagram summary of the GO terms associated with transcripts up-regulated in response to temperature stress in in hospite D. trenchii at 34 °C.*
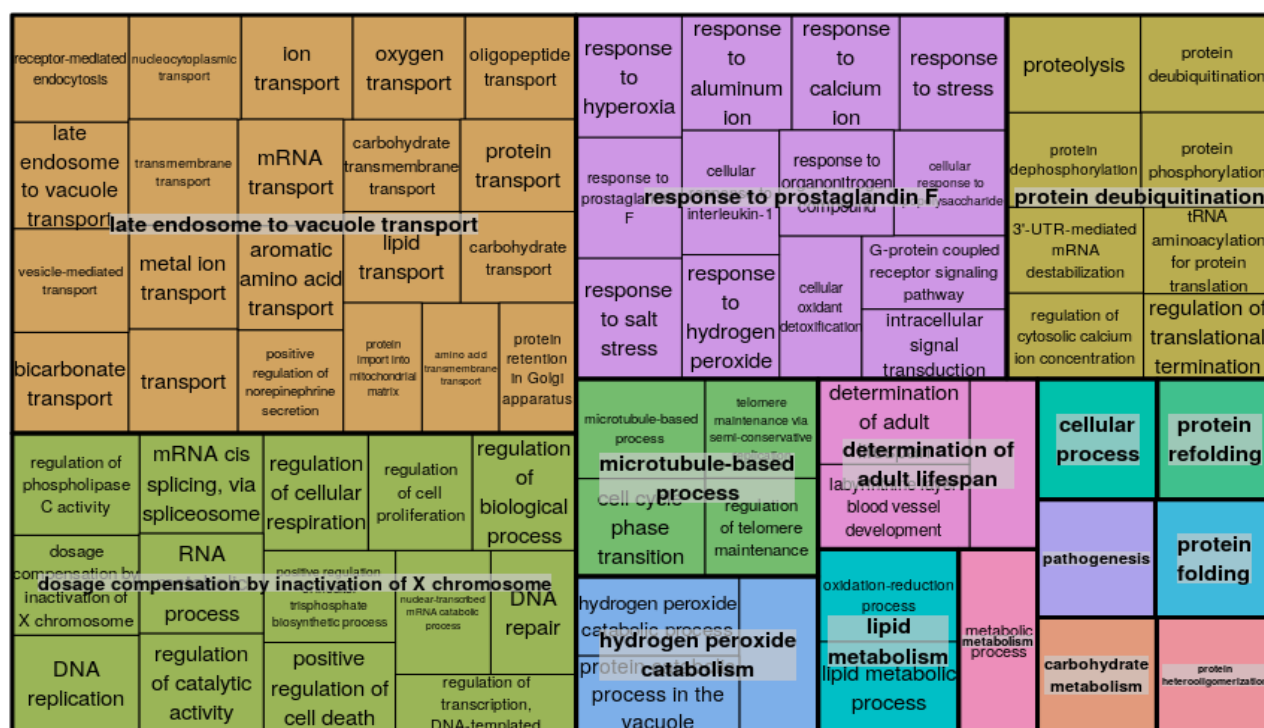
Supplementary Figure 8. REVIGO tree diagram summary of the GO terms associated

with transcripts down-regulated in response to temperature stress in in hospite D.

trenchii at 34 °C.

43

Supplementary Figure 9. *REVIGO tree diagram summary of the GO terms associated with transcripts up-regulated in response to temperature stress in free-living D. trenchii at 34 °C.*

747

748

Supplementary Figure 10. *REVIGO tree diagram summary of the GO terms*

associated with transcripts down-regulated in response to temperature stress in free-
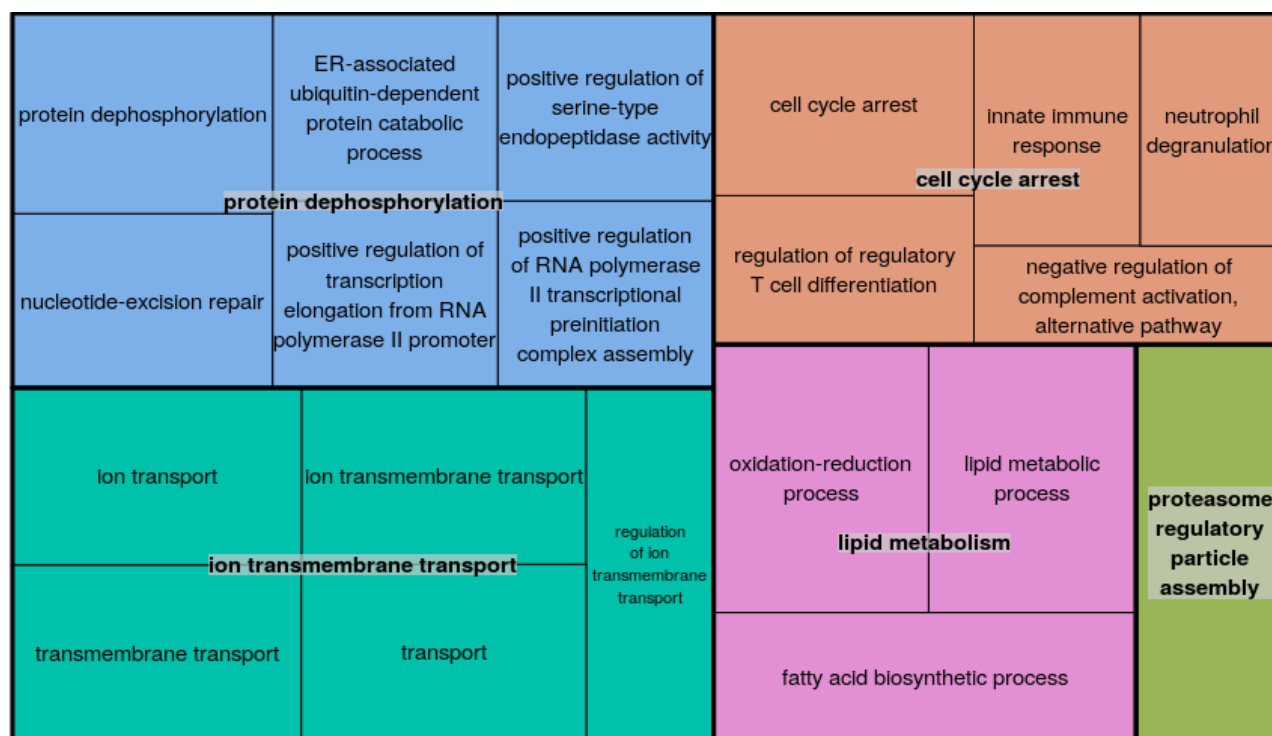
living D. trenchii at 34 °C.

752

Supplementary Figure 11. REVIGO tree diagram summary of the GO terms associated with transcripts that were up-regulated in response to symbiosis in D. trenchii at both 28 °C and 34 °C.
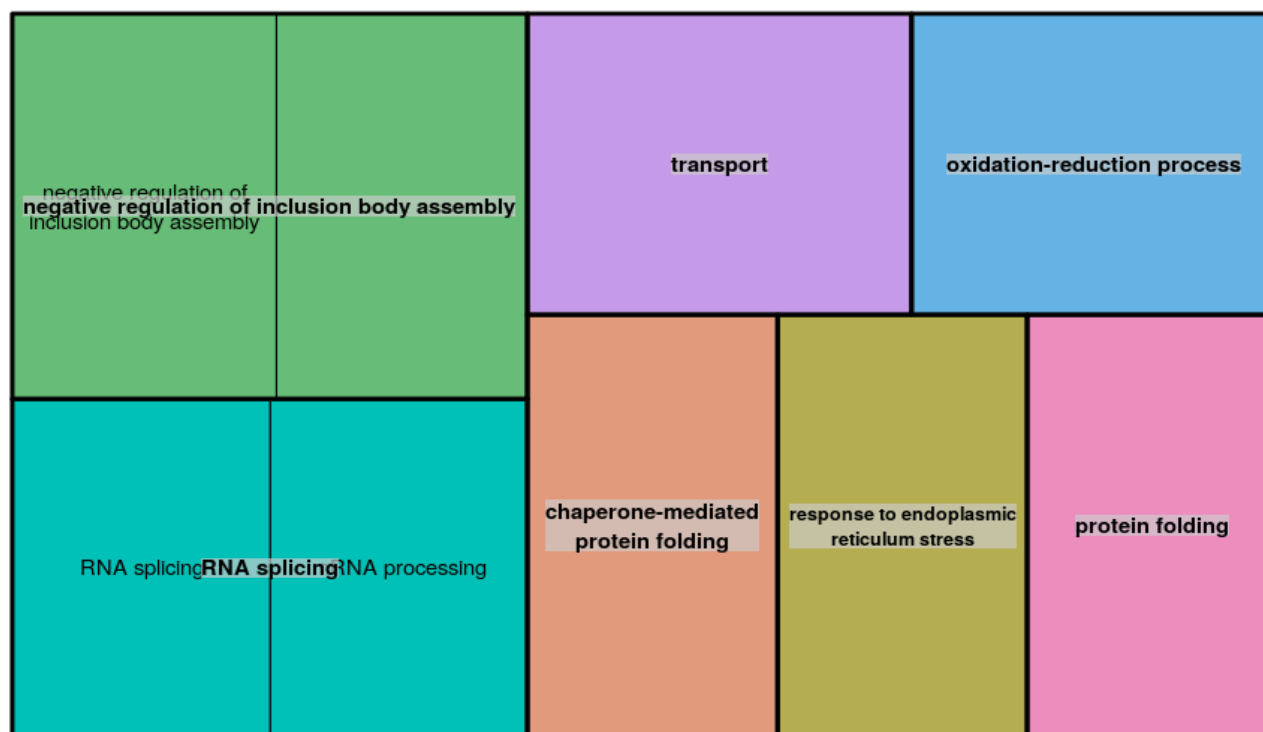
Supplementary Figure 12. *REVIGO tree diagram summary of the GO terms associated with transcripts that were down-regulated in response to symbiosis in D. trenchii at both 28 °C and 34 °C.*

47

Supplementary Figure 13. *REVIGO tree diagram summary of the GO terms associated with transcripts that were up-regulated in response to temperature stress in both free-living and symbiotic D. trenchii.*

Supplementary Figure 14. REVIGO tree diagram summary of the GO terms

associated with transcripts that were down-regulated in response to temperature stress

in both free-living and symbiotic D. trenchii.

770

Assembly metrics	
Total PE read sets after QC	526,545,945
Total PE read sets after QC (%)	81.5%
Assembly length (Mbp)	81.7
# Transcripts	85,168
Predicted ORF count	47,335
Genes annotated	28,531
Genes annotated (%)	60.3%
Longest gene length (bp)	8,088
Mean gene length (bp)	960.36
N50 (bp)	1,470
GC content (%)	0.55

771

772 **Supplementary Table 1.** *Assembly statistics for the D. trenchii assembly*

773

774

GO ID	Term	Annotated	Significant	FDR
GO:0003374	dynamin family protein polymerization involved in mitochondrial fission	6	3	0.0001
GO:0007089	traversing start control point of mitotic cell cycle	2	2	0.0003
GO:0018107	peptidyl-threonine phosphorylation	14	3	0.0017
GO:1904146	positive regulation of meiotic cell cycle process involved in oocyte maturation	4	2	0.0018
GO:0044341	sodium-dependent phosphate transport	5	2	0.0029
GO:0031649	heat generation	60	4	0.003
GO:0002024	diet induced thermogenesis	17	3	0.003
GO:0048266	behavioral response to pain	17	3	0.003
GO:0050960	detection of temperature stimulus involved in thermoreception	17	3	0.003

GO:0050965	detection of temperature stimulus involved in sensory perception	17	3	0.003
GO:0060083	smooth muscle contraction involved in micturition	17	3	0.003
GO:0060454	positive regulation of gastric acid secretion	17	3	0.003
GO:0071318	cellular response to ATP	17	3	0.003
GO:0071502	cellular response to temperature stimulus	17	3	0.003
GO:1901594	response to capsazepine	17	3	0.003
GO:0043154	negative regulation of cysteine-type endopeptidase activity involved in apoptotic process	18	3	0.0035
GO:0071468	cellular response to acidic pH	18	3	0.0035
GO:0090212	negative regulation of establishment of blood-brain barrier	18	3	0.0035
GO:0098703	calcium ion import across plasma membrane	18	3	0.0035
GO:0014047	glutamate secretion	19	3	0.0041

52

GO:0060337	type I interferon signaling pathway	19	3	0.0041
GO:0006975	DNA damage induced protein phosphorylation	6	2	0.0043
GO:0032264	IMP salvage	6	2	0.0043
GO:0001774	microglial cell activation	21	3	0.0055
GO:0090399	replicative senescence	7	2	0.006
GO:0050968	detection of chemical stimulus involved in sensory perception of pain	23	3	0.0072
GO:0030091	protein repair	8	2	0.0079
GO:0045957	negative regulation of complement activation, alternative pathway	8	2	0.0079
GO:1900004	negative regulation of serine-type endopeptidase activity	8	2	0.0079
GO:0045959	negative regulation of complement activation, classical pathway	9	2	0.0101
GO:0045589	regulation of regulatory T cell differentiation	10	2	0.0125

GO:0050954	sensory perception of mechanical stimulus	28	3	0.0125
GO:0046777	protein autophosphorylation	53	4	0.0136
GO:0071312	cellular response to alkaloid	31	3	0.0165
GO:0010044	response to aluminum ion	1	1	0.0175
GO:0032962	positive regulation of inositol trisphosphate biosynthetic process	1	1	0.0175
GO:0034696	response to prostaglandin F	1	1	0.0175
GO:0036466	synaptic vesicle recycling via endosome	1	1	0.0175
GO:0046519	sphingoid metabolic process	1	1	0.0175
GO:0051482	positive regulation of cytosolic calcium ion concentration involved in phospholipase C-activating G-protein coupled signaling pathway	1	1	0.0175
GO:0060716	labyrinthine layer blood vessel development	1	1	0.0175
GO:0070058	mitochondrion morphogenesis	1	1	0.0175

GO ID	Description			
4				
GO:009014 9	mitochondrial membrane fission	1	1	0.0175
GO:190024 4	positive regulation of synaptic vesicle endocytosis	1	1	0.0175
GO:190457 9	cellular response to thapsigargin	1	1	0.0175
GO:190539 5	response to flavonoid	1	1	0.0175
GO:199091 0	response to hypobaric hypoxia	1	1	0.0175
GO:200030 2	positive regulation of synaptic vesicle exocytosis	1	1	0.0175
GO:000600 2	fructose 6-phosphate metabolic process	12	2	0.0179
GO:003112 2	cytoplasmic microtubule organization	12	2	0.0179
GO:003296 8	positive regulation of transcription elongation from RNA polymerase II promoter	12	2	0.0179
GO:001507 4	DNA integration	33	3	0.0195
GO:000039	mRNA splicing, via spliceosome	90	5	0.0205

8				
GO:0090307	mitotic spindle assembly	13	2	0.0209
GO:0031098	stress-activated protein kinase signaling cascade	107	3	0.0242
GO:0032507	maintenance of protein location in cell	15	2	0.0274
GO:0043312	neutrophil degranulation	66	4	0.0281
GO:0051289	protein homotetramerization	66	4	0.0281
GO:0007286	spermatid development	16	2	0.031
GO:0007344	pronuclear fusion	2	1	0.0346
GO:0010569	regulation of double-strand break repair via homologous recombination	2	1	0.0346
GO:0010701	positive regulation of norepinephrine secretion	2	1	0.0346
GO:0010767	regulation of transcription from RNA polymerase II promoter in response to UV-induced DNA damage	2	1	0.0346

GO:0016325	oocyte microtubule cytoskeleton organization	2	1	0.0346
GO:0016559	peroxisome fission	2	1	0.0346
GO:0019509	L-methionine salvage from methylthioadenosine	2	1	0.0346
GO:0023016	signal transduction by trans-phosphorylation	2	1	0.0346
GO:0032298	positive regulation of DNA-dependent DNA replication initiation	2	1	0.0346
GO:0034311	diol metabolic process	2	1	0.0346
GO:0036438	maintenance of lens transparency	2	1	0.0346
GO:0045196	establishment or maintenance of neuroblast polarity	2	1	0.0346
GO:0045450	bicoid mRNA localization	2	1	0.0346
GO:0061003	positive regulation of dendritic spine morphogenesis	2	1	0.0346
GO:0071476	cellular hypotonic response	2	1	0.0346
GO:0072422	signal transduction involved in G2	2	1	0.0346

5	*DNA damage checkpoint*			
GO:0090188	*negative regulation of pancreatic juice secretion*	*2*	*1*	*0.0346*
GO:0090200	*positive regulation of release of cytochrome c from mitochondria*	*2*	*1*	*0.0346*
GO:1900063	*regulation of peroxisome organization*	*2*	*1*	*0.0346*
GO:1905408	*negative regulation of creatine transmembrane transporter activity*	*2*	*1*	*0.0346*
GO:2000650	*negative regulation of sodium ion transmembrane transporter activity*	*2*	*1*	*0.0346*
GO:2000681	*negative regulation of rubidium ion transport*	*2*	*1*	*0.0346*
GO:0051570	*regulation of histone H3-K9 methylation*	*17*	*2*	*0.0347*
GO:0034605	*cellular response to heat*	*42*	*3*	*0.0366*
GO:0000289	*nuclear-transcribed mRNA poly(A) tail shortening*	*18*	*2*	*0.0387*
GO:0071356	*cellular response to tumor necrosis factor*	*126*	*6*	*0.0414*
GO:0046605	*regulation of centrosome cycle*	*19*	*2*	*0.0427*

GO:0045429	positive regulation of nitric oxide biosynthetic process	45	3	0.0436
GO:0043434	response to peptide hormone	76	4	0.0437

775

776 **Supplementary Table 2.** Gene ontology enrichment analysis results comparing the

777 transcriptional profiles of D. trenchii when in hospite at 28 °C to the free-living stage at

778 28 °C

GO ID	Term	Annotated	Significant	FDR
GO:0003341	cilium movement	36	13	5.10E-11
GO:0001539	cilium or flagellum-dependent cell motility	27	9	1.20E-07
GO:0009250	glucan biosynthetic process	61	10	0.00012
GO:1904146	positive regulation of meiotic cell cycle process involved in oocyte maturation	4	3	0.00014
GO:0007089	traversing start control point of mitotic cell cycle	2	2	0.00109
GO:0015671	oxygen transport	25	5	0.00117
GO:0015701	bicarbonate transport	26	5	0.00141
GO:0045957	negative regulation of complement activation, alternative pathway	8	3	0.00177
GO:1900004	negative regulation of serine-type endopeptidase activity	8	3	0.00177
GO:0045959	negative regulation of complement activation, classical pathway	9	3	0.00258

GO:0045589	regulation of regulatory T cell differentiation	10	3	0.0036
GO:0042744	hydrogen peroxide catabolic process	32	5	0.00368
GO:0006865	amino acid transport	123	12	0.00569
GO:0007157	heterophilic cell-cell adhesion via plasma membrane cell adhesion molecules	12	3	0.00629
GO:0051965	positive regulation of synapse assembly	13	3	0.00797
GO:0070317	negative regulation of G0 to G1 transition	5	2	0.01017
GO:0045454	cell redox homeostasis	134	10	0.01322
GO:0003374	dynamin family protein polymerization in mitochondrial fission	6	2	0.01493
GO:0006452	translational frameshifting	6	2	0.01493
GO:1902475	L-alpha-amino acid transmembrane transport	6	2	0.01493
GO:0050770	positive regulation of dendrite	7	2	0.02045

5	morphogenesis			
GO:0006813	potassium ion transport	115	8	0.02218
GO:0030091	protein repair	8	2	0.02668
GO:0098869	cellular oxidant detoxification	53	5	0.02997
GO:0010044	response to aluminum ion	1	1	0.03302
GO:0032962	positive regulation of inositol trisphosphate biosynthetic process	1	1	0.03302
GO:0034696	response to prostaglandin F	1	1	0.03302
GO:0035444	nickel cation transmembrane transport	1	1	0.03302
GO:0036466	synaptic vesicle recycling via endosome	1	1	0.03302
GO:0042908	xenobiotic transport	1	1	0.03302
GO:0051482	positive regulation of cytosolic calcium ion concentration involved in phospholipase C-activating G-protein coupled signaling pathway	1	1	0.03302

GO:0060716	labyrinthine layer blood vessel development	1	1	0.03302
GO:0070407	oxidation-dependent protein catabolic process	1	1	0.03302
GO:0070584	mitochondrion morphogenesis	1	1	0.03302
GO:0072432	response to G1 DNA damage checkpoint signaling	1	1	0.03302
GO:0090149	mitochondrial membrane fission	1	1	0.03302
GO:0090296	regulation of mitochondrial DNA replication	1	1	0.03302
GO:1900244	positive regulation of synaptic vesicle endocytosis	1	1	0.03302
GO:1904579	cellular response to thapsigargin	1	1	0.03302
GO:1905395	response to flavonoid	1	1	0.03302
GO:1990910	response to hypobaric hypoxia	1	1	0.03302
GO:2000302	positive regulation of synaptic vesicle exocytosis	1	1	0.03302
GO:0006898	receptor-mediated endocytosis	104	8	0.03359

8				
GO:005129 1	*protein heterooligomerization*	*55*	*5*	*0.03447*
GO:000028 9	*nuclear-transcribed mRNA poly(A) tail shortening*	*18*	*3*	*0.0489*

779

780 **Supplementary Table 3.** *Gene ontology enrichment analysis results comparing the*

781 *transcriptional profiles of D. trenchii when in hospite at 34 °C to the free-living stage at*

782 *34 °C.*

783

GO ID	Term	Annotated	Significant	FDR
GO:0042545	cell wall modification	2	1	0.01
GO:0007218	neuropeptide signaling pathway	3	1	0.015
GO:0019594	mannitol metabolic process	3	1	0.015
GO:0060012	synaptic transmission, glycinergic	3	1	0.015
GO:0070247	regulation of natural killer cell apoptotic process	3	1	0.015
GO:0071266	de novo' L-methionine biosynthetic process	3	1	0.015
GO:1990001	inhibition of cysteine-type endopeptidase activity involved in apoptotic process	4	1	0.02
GO:0007023	post-chaperonin tubulin folding pathway	5	1	0.025
GO:0015801	aromatic amino acid transport	5	1	0.025
GO:0045899	positive regulation of RNA polymerase II transcriptional preinitation complex assembly	6	1	0.03
GO:0000186	activation of MAPKK activity	7	1	0.034
GO:0032801	receptor catabolic process	8	1	0.039
GO:0045957	negative regulation of complement activation, alternative pathway	8	1	0.039

GO:1900004	negative regulation of serine-type endopeptidase activity	8	1	0.039
GO:0045959	negative regulation of complement activation, classical pathway	9	1	0.044
GO:0006072	glycerol-3-phosphate metabolic process	10	1	0.049
GO:0045589	regulation of regulatory T cell differentiation	10	1	0.049
GO:0060056	mammary gland involution	10	1	0.049

784

785 **Supplementary Table 4.** *Gene ontology enrichment analysis results comparing the*

786 *transcriptional profiles of D. trenchii when free-living at 34 °C to the free-living stage at*

787 *28 °C.*

788

GO ID	Term	Annotated	Significant	FDR
GO:001002 1	amylopectin biosynthetic process	2	1	0.014
GO:004545 4	cell redox homeostasis	134	4	0.015
GO:000597 8	glycogen biosynthetic process	30	2	0.019
GO:000752 3	larval visceral muscle development	3	1	0.021
GO:003605 9	nephrocyte diaphragm assembly	3	1	0.021
GO:004683 2	negative regulation of RNA export from nucleus	3	1	0.021
GO:007110 8	protein K48-linked deubiquitination	3	1	0.021
GO:000715 6	homophilic cell adhesion via plasma membrane adhesion molecules	4	1	0.028
GO:007053 6	protein K63-linked deubiquitination	4	1	0.028
GO:009720 6	nephrocyte filtration	5	1	0.035
GO:000642	glycyl-tRNA aminoacylation	6	1	0.042

6				
GO:0042128	*nitrate assimilation*	*6*	*1*	*0.042*
GO:0045899	*positive regulation of RNA polymerase II transcriptional preinitiation complex assembly*	*6*	*1*	*0.042*
GO:0051292	*nuclear pore complex assembly*	*6*	*1*	*0.042*
GO:0006474	*N-terminal protein amino acid acetylation*	*7*	*1*	*0.049*
GO:0006542	*glutamine biosynthetic process*	*7*	*1*	*0.049*
GO:0007076	*mitotic chromosome condensation*	*7*	*1*	*0.049*

789

790 **Supplementary Table 5.** *Gene ontology enrichment analysis results comparing the*

791 *transcriptional profiles of D. trenchii when in hospite at 34 °C to symbiosis at 28 °C.*

792

793

794

795

796

797